THE JOURNAL OF BIOLOGICAL CHEMISTRY VOL. 289, NO. 19, pp. 13243–13258, May 9, 2014

Physiological IgM Class Catalytic Antibodies Selective for Transthyretin Amyloid*

Received for publication, February 10, 2014, and in revised form, March 13, 2014 Published, JBC Papers in Press, March 19, 2014, DOI 10.1074/jbc.M114.557231

Stephanie A. Planque[‡], Yasuhiro Nishiyama[‡], Mariko Hara[‡], Sari Sonoda[‡], Sarah K. Murphy[‡], Kenji Watanabe[‡], Yukie Mitsuda[‡], Eric L. Brown[§], Richard J. Massey[¶], Stanley R. Primmer[‖], Brian O'Nuallain[**], and Sudhir Paul[‡1]

*From the [‡]Chemical Immunology Research Center, Department of Pathology and Laboratory Medicine, University of Texas-Houston Medical School, Houston, Texas 77030, the [§]Center for Infectious Diseases, University of Texas School of Public Health, Houston, Texas 77030, [¶]Covalent Bioscience Inc., Houston, Texas 77054, the [‖]Supercentenarian Research Foundation, Lauderhill, Florida 33319, and the **Center for Neurologic Diseases, Brigham and Women's Hospital and Harvard Medical School, Boston, Massachusetts 02115*

Background: Some antibodies express serine protease activity. Transthyretin misfolding causes accumulation of pathogenic amyloid.
Results: Constitutively produced IgM but not IgG class antibodies selectively hydrolyzed and dissolved misfolded transthyretin without hydrolyzing physiologically folded transthyretin. Some IgMs were oligoreactive with amyloids and superantigens.
Conclusion: Catalytic IgMs may clear misfolded TTR and delay amyloidosis.
Significance: The innate antibody repertoire is a source of selective catabodies to toxic proteins.

Peptide bond-hydrolyzing catalytic antibodies (catabodies) could degrade toxic proteins, but acquired immunity principles have not provided evidence for beneficial catabodies. Transthyretin (TTR) forms misfolded β-sheet aggregates responsible for age-associated amyloidosis. We describe nucleophilic catabodies from healthy humans without amyloidosis that degraded misfolded TTR (misTTR) without reactivity to the physiological tetrameric TTR (phyTTR). IgM class B cell receptors specifically recognized the electrophilic analog of misTTR but not phyTTR. IgM but not IgG class antibodies hydrolyzed the particulate and soluble misTTR species. No misTTR-IgM binding was detected. The IgMs accounted for essentially all of the misTTR hydrolytic activity of unfractionated human serum. The IgMs did not degrade non-amyloidogenic, non-superantigenic proteins. Individual monoclonal IgMs (mIgMs) expressed variable misTTR hydrolytic rates and differing oligoreactivity directed to amyloid β peptide and microbial superantigen proteins. A subset of the mIgMs was monoreactive for misTTR. Excess misTTR was dissolved by a hydrolytic mIgM. The studies reveal a novel antibody property, the innate ability of IgMs to selectively degrade and dissolve toxic misTTR species as a first line immune function.

Higher organisms possess a structurally diverse innate repertoire of antibody variable domains (V domains)[2] that was shaped by evolutionary selection pressures imposed by foreign antigens and self-antigens over millions of years. The diversity is supplemented by somatic randomization of the V domains by acquired immunity processes, which enables selection of V domains with noncovalent antigen binding activity over a few weeks upon contact with an antigen. Catalytic antibodies (catabodies) with a promiscuous peptide bond hydrolytic activity, on the other hand, are produced as an innate property of B cells, requiring no exposure to the antigen (1, 2). The proteolytic activity was traced to serine protease-like sites in the germ line antibody V-regions, suggesting an ancient origin of the catabodies (3–6). Humans produce catabodies selective for amyloid β peptide (Aβ) (7). Immune tolerance mechanisms in fetal and adult life are thought to suppress synthesis of autoantibodies to essential self-proteins. When produced, subsets of autoantibodies express autoantigen-selective catalytic activities (8–10). Provided that catabodies discriminate between individual peptide antigens, they hold potential for specific and permanent destruction of toxic self-antigens.

Many proteins can misfold into the amyloid state (11). Soluble transthyretin (TTR) is found in large amounts in blood (~0.3 mg/ml) in its physiological, homotetrameric state (phyTTR) as a carrier protein for thyroid hormones and the retinol-retinol binding protein complex (12). Misfolded β-sheet-containing aggregates are generated from TTR (collectively designated misTTR states; Table 1), a process involving formation of a TTR monomer, destabilization of the phyTTR dimer-dimer interface, and growth of soluble misTTR oligo-

* This work was supported, in whole or in part, by National Institutes of Health Grant U01AG033183. This work was also supported by the SENS Research Foundation. The Flow Cytometry Core at the Baylor College of Medicine is funded by National Institutes of Health Grants S10RR024574, AI036211, and P30CA125123. Stephanie Planque, Yasuhiro Nishiyama, Eric Brown, Richard Massey, and Sudhir Paul have a financial interest in Covalent Bioscience, Inc. and patents concerning catalytic antibodies.

[1] To whom correspondence should be addressed: Chemical Immunology Research Center, Dept. of Pathology and Laboratory Medicine, University of Texas-Houston Medical School, 6431 Fannin, Houston, TX 77030. Tel.: 713-500-5347; Fax: 713-500-0574; E-mail: Sudhir.Paul@uth.tmc.edu.

[2] The abbreviations used are: V domain, V_H domain, and V_L domain, variable domain, heavy chain variable domain, and light chain variable domain, respectively; AMC, aminomethylcoumarin; Ab, antibody; Aβ, amyloid β peptide; Aβ42, Aβ 1–42; Aβ40, Aβ 1–40; BCR, B cell receptor; C domain, constant domain; catabody, catalytic antibody; CDR, complementarity-determining region; misTTR, misfolded TTR; E-misTTR, electrophilic misTTR; phyTTR, physiological TTR; E-phyTTR, electrophilic phyTTR; MMP9, matrix metalloproteinase-9; mIgM, monoclonal IgM; PECy7, phycoerythrin cyanine 7; SA, streptavidin; pIgM, polyclonal IgM; SAP, serum amyloid P component; SSA, senile systemic amyloidosis; ThT, Thioflavin-T; TTR, transthyretin.

TABLE 1
Properties of phyTTR and misTTR

Property	phyTTR	misTTR
Solubility	Soluble	Particulate and soluble
Aggregate subunit composition	4-Mer	Variable (2 to millions)
Aggregate stability in boiling SDS	Dissociates into 1-mers	Dissociates into 1-mers
Aggregate stability in SDS without boiling	Remains as 4-mers[a]	Dissociates into 1-mers[a]
Biological distribution	Blood, tissue ISF[b]	Blood, tissue ISF, tissue amyloid
Pathogenicity	None	Cellular toxicity, anatomic disruption

[a] Data from Refs. 30–32.
[b] ISF, interstitial fluid.

mers into fibrillar amyloid (13–15). Small misTTR amounts are probably formed continuously as basal byproducts of alternate TTR folding pathways. Initial evidence for the existence of blood-borne misTTR species is available (16). Dysregulated protein misfolding during normal aging processes causes increased TTR amyloid deposition in several tissues (12). TTR amyloid deposition in the tenosynovium is associated with carpal tunnel syndrome in middle-aged humans (17). TTR amyloidosis in the heart, lung, stomach, kidney, and other tissues causes organ failure in senile systemic amyloidosis (SSA), a disease affecting >10% humans over age 70 years (12, 18–20). In addition, mutations in the TTR gene cause early onset familial TTR amyloidosis (21). Amyloid deposits cause architectural and functional tissue damage, and soluble misTTR aggregates exert direct cytotoxic effects. No approved pharmacological treatment for SSA is available, but anti-transthyretin RNAi reagents are undergoing clinical trials (22), and a small molecule drug that interacts with the thyroxine binding site of TTR may help relieve symptoms of polyneuropathy in familial TTR amyloidosis (23). Reversibly binding antibodies that can clear amyloids by phagocytosis of the immune complexes have been proposed as potential therapeutic reagents (24–26). We report IgM class catabodies produced by healthy humans that hydrolyze misTTR but not phyTTR. The catabodies can be conceived as homeostatic mediators that destroy TTR amyloid and its precursor misfolded TTR forms without interfering in the physiological functions of TTR.

MATERIALS AND METHODS

Antibodies—Human studies were approved by the Committee for the Protection of Human Subjects, University of Texas Health Science Center (Houston, TX). Individual or pooled polyclonal IgM, IgG, and IgA class antibodies were purified from sera of 12 healthy humans without amyloidosis or autoimmune disease (33 ± 7 years in age) by acid elution (pH 2.7) from columns of immobilized anti-human IgM antibodies, Protein G, and anti-human IgA antibodies (1, 27). The antibody preparations were free of detectable non-antibody proteins judged by SDS-gel electrophoresis and immunoblotting with specific antibodies to IgM, IgG, and IgA. For evaluation of aging effects, IgMs were purified from non-aged humans (<35 years in age) or aged humans (>70 years) of either gender without amyloidosis or autoimmune disease. The monoclonal IgM (mIgM) panel purified from Waldenström macroglobulinemia patients was described (our laboratory codes 1800-1804, 1806, 1809-1811, 1813, 1814, 1816-1819, and Yvo) (2). Unfractionated human serum was pooled from 10 healthy humans (36 ± 5 years in age). To prepare antibody-free serum, the pooled serum was adsorbed sequentially on the anti-IgM, Protein G, and anti-IgA columns (residual IgM, IgA, and IgG estimated by ELISA were 0.05, 0.007, and 0.003%, respectively) (28). FPLC gel filtration of the unfractionated serum pool (70 μl) was on a Superose-6 column (GE Healthcare; flow rate, 0.1 ml/min) in 10 mM sodium phosphate, pH 7.4, 137 mM NaCl, 2.7 mM KCl (PBS) containing 0.1 mM CHAPS. The Aβ-hydrolyzing recombinant catalytic antibody fragment (clone 2E6) was purified as described (29). Nominal molecular mass was computed by comparison with protein markers (a reference 900-kDa mIgM and 1.4–670-kDa markers from Bio-Rad). Total protein was measured by the Micro BCA™ method (Thermo Fisher Scientific). Cell surface IgMs were analyzed using the purified peripheral blood B cells from a 25-year-old human subject without amyloidosis (B cell negative selection kit, Miltenyi (Auburn, CA); viability, 90–95%; >95% purity determined by staining with phycoerythrin-conjugated mouse antibody to human CD19 (BD Pharmingen) and flow cytometry).

Aggregated TTR—Wild type, purified TTR from human plasma (Cell Sciences, Canton, MA) was labeled with ^{125}I (^{125}I-TTR) using 1,3,4,6-tetrachloro-3α,6α-diphenylglycouril (Thermo Fisher Scientific), followed by removal of free ^{125}I by gel filtration (BioSpin-6 column; Bio-Rad). The TTR or ^{125}I-TTR solutions were preaggregated in PBS containing 1 mM EDTA (0.4 mg of TTR/ml, 28.6 μM; molar TTR concentrations computed from the monomer TTR mass, 14 kDa) by acidification with an equal volume of 200 mM sodium acetate, pH 4.2, 100 mM KCl, 1 mM EDTA, followed by incubation for 5 days at 37 °C (15). After exchanging the buffer to PBS containing 0.1 mM CHAPS (PBS/CHAPS) with an Ultra-4 centrifugal filter (EMD Millipore, Billerica, MA), the aggregated TTR (~14 μM) was stored in aliquots at −80 °C. Non-aggregated TTR is composed of soluble physiological tetramers, and the aggregation reaction produces soluble and particulate misfolded TTR (13–15). Aggregation was monitored by turbidimetry at 400 nm (10-mm path length; Cary 50 spectrophotometer, Agilent, Santa Clara, CA). In addition, binding of TTR (100 μl, 0.1 mg/ml) to thioflavin T (ThT) was determined by mixing with ThT (2.5 μl, 0.6 mM in PBS containing 0.1 mM CHAPS and 12% dimethyl sulfoxide) and measurement of fluorescence emission (λ_{em} = 485 nm, λ_{ex} = 440 nm, 600-V photomultiplier voltage; Varian Cary Eclipse fluorimeter). The supernatant and pellet containing the soluble and particulate TTR species, respectively, were separated by centrifugation (17,000 × *g*, 20 min).

The phyTTR and misTTR states were dissociated into monomers (14 kDa) by boiling test samples (10 min) after mixing with a one-fifth volume of 10% SDS in electrophoresis

buffer (0.313 M Tris-HCl, pH 6.8, containing 17% 2-mercaptoethanol, 50% glycerol, and 0.025% bromphenol blue). Electrophoresis was in 16.5% polyacrylamide Criterion gels (Bio-Rad) in 100 mM Tris-Tricine, pH 8.3, containing 0.1% SDS. Protein mass was computed by comparison with standard proteins (14–94 and 1.4–26.6 kDa ladders; Bio-Rad). The phyTTR and misTTR states were distinguished by electrophoresing non-boiled test samples treated with 10% SDS treatment in non-reducing buffer. The 54-kDa phyTTR 4-mers dissociate into 1-mers by upon boiling in SDS but remain undissociated in SDS at room temperature, whereas SDS treatment at room temperature is sufficient to dissociate misTTR aggregates into 14-kDa 1-mers (30–32). Radioactive TTR bands were detected with a Cyclone Plus PhosphorImager (PerkinElmer Life Sciences; 30–120-min exposure, supersensitive storage screen; minimum detectable radioactivity + 3 S.D. values, 500 cpm; linear detection up to 867,000 cpm). The percentage of misTTR content of preaggregated ^{125}I-TTR was determined by densitometry as follows, 100 × (14 kDa band intensity)/(sum of 14 and 54 kDa band intensities), where the band intensity was in arbitrary volume units (ImageJ software, National Institutes of Health, Bethesda, MD).

The biotinylated, electrophilic analogs of misTTR (E-misTTR) and phyTTR (E-phyTTR) were prepared as described (33) (6.0 and 0.1 mol of phosphonate and biotin, respectively, per mol of misTTR; 3.9 and 1.5 mol of phosphonate groups and biotin, respectively, per mol of phyTTR). The starting material for E-misTTR preparation was the particulate misTTR in PBS/CHAPS recovered by centrifugation (30 min, 75,000 × *g*).

Proteolysis—All tests were done in duplicate or as specified. Non-aggregated or preaggregated ^{125}I-TTR (100 nM monomer equivalents) was incubated with purified antibodies in PBS/CHAPS (20 μl). The boiled or non-boiled reaction mixtures were analyzed by SDS-gel electrophoresis (8,930–17,110 cpm/lane). Depletion of the 1-mer TTR band (14 kDa) and appearance of lower mass products were quantified by densitometry. Antibody (Ab) hydrolytic activity was computed in units of nM misTTR hydrolyzed/μg of antibody/h ((A nM × (1 − [14 kDa_{Ab}]/[14 kDa_{Dil}]))/(μg of Ab in the reaction mixture/Ab treatment time in h), where A is the initial misTTR concentration (total TTR concentration × % misTTR content) if non-boiled samples were analyzed or the total TTR concentration (misTTR + phyTTR) if boiled samples were analyzed, and [14 kDa_{Ab}] and [14 kDa_{Dil}] are the 14 kDa band intensities after antibody and diluent treatment, respectively). For data reported in this format, variations of the misTTR hydrolysis rate up to 2.4-fold are predicted because of varying misTTR content in different preaggregated TTR preparations (29–70%).

Hydrolysis of non-radiolabeled TTR bands stained with silver was quantified similarly. Protease inhibitors were tested at concentrations sufficient for complete inhibition of metalloproteases (EDTA, 2 mM; 1,10-phenanthroline, 1 mM), cysteine proteases (iodoacetamide, 0.1 mM), acid proteases (pepstatin A, 1 μM), and serine proteases (phosphonate 1, 0.1 mM) (34). Phosphonate 1 ((diphenyl *N*-[6-(biotinamido)hexanoyl]amino(4-amidinophenyl)methane phosphonate)) is an active site-directed inhibitor of nucleophilic catabodies (35). Alkylation of the free -SH group in TTR was avoided by pretreating antibodies with iodoacetamide (60 min) and removing this reagent prior to the proteolysis assay (BioSpin-6 gel filtration column). Inhibition of antibody proteolysis by serum amyloid P component (SAP; Calbiochem, Billerica, MA) was tested under conditions reported to reduce TTR sensitivity to digestion by human matrix metalloproteinase-9 (MMP9 from human neutrophils (EMD Millipore); preaggregated ^{125}I-TTR containing 1 μM misTTR pretreated with 0.55 μM SAP or control albumin for 2 h in 10 mM Tris-HCl, pH 8.0, 138 mM NaCl, 2 mM $CaCl_2$) (36). MMP9 was activated by incubation for 3 h with 5 mM 4-aminophenylmercuric acetate, and the enzyme was recovered by gel filtration for hydrolysis tests.

Hydrolysis of fluorigenic *N*-*t*-butoxycarbonyl-*O*-benzyl-Glu-Ala-Arg-7-amino-4-methylcoumarin (EAR-AMC) and amyloid β peptide 1–40 (Aβ40) was tested as described previously (7). ^{125}I-Aβ 1–42 (Aβ42, 90 μg; EZBiolab (Carmel, IN)) was radiolabeled as described for TTR, and free ^{125}I was removed using a Sep-Pak Vac C18 cartridge (37). The fibrillar Aβ42 substrate (2.3×10^7 cpm/μmol Aβ42) was prepared by co-aggregating ^{125}I-Aβ42 (0.7×10^9 cpm in 1,1,1,3,3,3-hexafluoro-2-propanol, 0.1 ml) and Aβ42 (1 mg; 5 mM solution in dimethyl sulfoxide). The mixture was diluted to 50 μM Aβ42 with PBS and incubated for 92 h (37 °C), and the fibrillar ^{125}I-Aβ42 was collected by centrifugation (17,000 × *g*, 20 min). Following digestion of fibrillar ^{125}I-Aβ42 with antibodies (30,000 cpm, 16 h), the reaction mixtures were treated with formic acid (60%, v/v) and fractionated on a Superdex peptide gel filtration column (GE Healthcare) in 60% formic acid. Hydrolysis of these biotinylated proteins was measured by SDS-gel electrophoresis and staining with streptavidin-peroxidase as described (2) (molar biotin/protein ratio in parentheses): gp120 from HIV strain MN (1.6), *Staphylococcus aureus* Protein A (5.0), bovine serum albumin (9.0), extracellular domain of human epidermal growth factor receptor (2.3), bovine thyroglobulin (26.0), human transferrin (5.4), and ovalbumin (1.6).

Binding—Preaggregated ^{125}I-TTR (25,000 cpm; 100 nM TTR, 60% misTTR content) was incubated (16 h) with or without IgMs (130 μg/ml) in 40 μl in PBS/CHAPS. The soluble and particulate fractions were separated by centrifugation (20 min, 17,000 × *g*), and the particulate fraction was resuspended in 40 μl of PBS/CHAPS and treated separately for 1 h with the immobilized anti-human IgM gel (50 μl settled gel), and the mixtures were centrifuged (5 min, 500 × g), the gel was washed with 250 μl of PBS/CHAPS, and radioactivity in supernatant (unbound ^{125}I-TTR) and gel (bound ^{125}I-TTR) was measured. The percentage of bound ^{125}I-TTR was computed as 100 × (cpm total binding − cpm nonspecific binding)/(cpm ^{125}I-TTR in the initial reaction mixture), where "total binding" refers to the binding in IgM-containing reaction mixtures, and "nonspecific binding" refers to binding in the reactions containing PBS/CHAPS instead of IgMs.

For cell binding studies, large E-misTTR particles were removed by centrifugation (400 × *g*, 10 min), and the E-misTTR did not contain flow cytometrically detectable particles. B cells were pretreated with mouse serum (1% in PBS, 10 min) to saturate Fc receptors and with the Endogenous Avidin/Biotin Blocking kit to saturate cellular biotin as recommended by the manufacturer (Abcam, Cambridge, MA). The cells

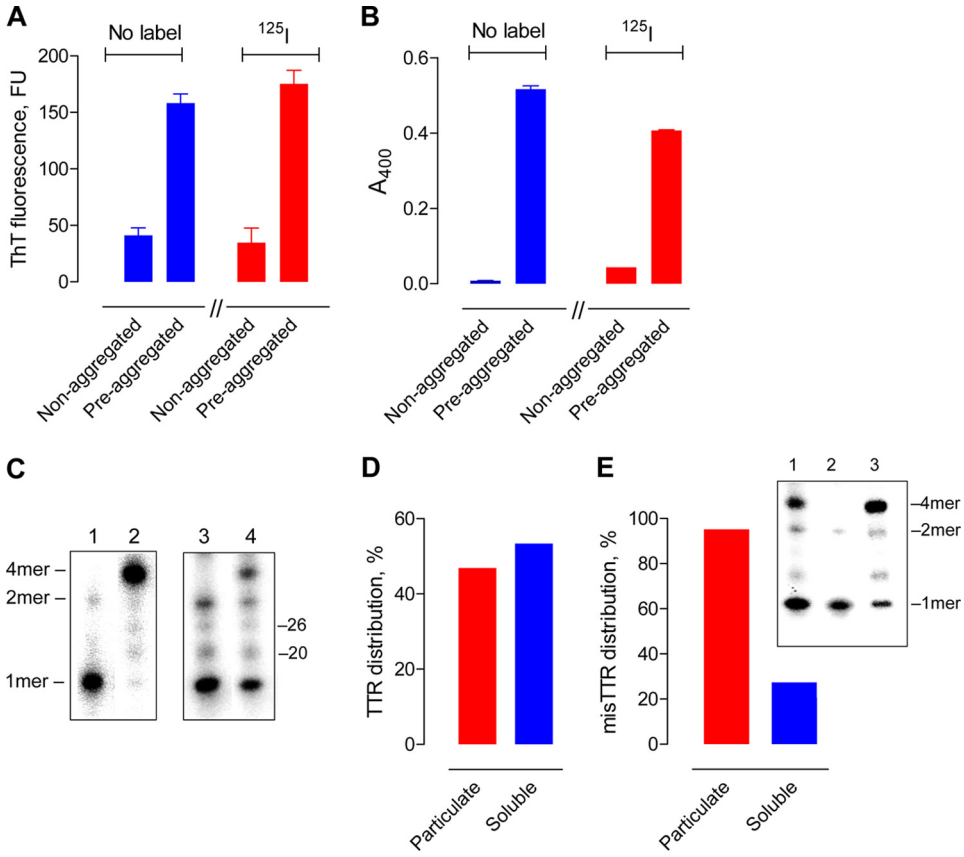

FIGURE 1. **Preaggregated and non-aggregated TTR properties.** *A*, ThT binding. ThT fluorescence values for non-radiolabeled TTR (*no label*) and ^{125}I-TTR (*^{125}I*) were small compared with TTR aggregated over 5 days (TTR, 7.1 μM; ThT, 15 μM). *B*, turbidity. The turbidity of non-radiolabeled TTR (*no label*) and ^{125}I-TTR (*^{125}I*) was marginal compared with the TTR aggregated over 5 days. *C*, SDS-gel electrophoresis. *Left box*, non-aggregated ^{125}I-TTR without (*lane 2*) or with boiling (*lane 1*). *Right box*, preaggregated ^{125}I-TTR without (*lane 4*) or with boiling (*lane 3*). Bands labeled 4mer, 2mer, and 1mer are the tetramer (54 kDa), dimer (27 kDa), and monomer (14 kDa), respectively. Minor 20 and 26 kDa bands are impurities from the source TTR (<0.5%). The 4-mer phyTTR species is dominant in non-boiled, non-aggregated TTR, whereas the 1-mer derived from soluble and insoluble misTTR is present in large amounts in the non-boiled, preaggregated TTR. misTTR content of the preaggregated and non-aggregated ^{125}I-TTR preparation, respectively, is 70 and <0.5%. *D*, TTR distribution in particulate and soluble fractions. Nearly equivalent radioactivity amounts from preaggregated ^{125}I-TTR were recovered in the pellet (particulate fraction) and supernatant (soluble fraction) obtained by centrifugation. *E*, misTTR distribution in particulate and soluble TTR fractions. The non-boiled particulate and soluble fractions prepared from preaggregated ^{125}I-TTR contained the radioactive 1-mer band derived from misTTR as the majority and minority species, respectively. Plotted values computed as 100 × (1-mer band intensity/sum of 1-mer and 4-mer band intensities). *Inset*, *lane 1* shows preaggregated ^{125}I-TTR without separation into particulate and soluble fractions (radioactivity in 1-mer and 4-mer bands, respectively, 43 and 57%). The 1-mer band is dominant in particulate ^{125}I-TTR (95% of total radioactivity; *lane 2*) and is also present in smaller amounts in soluble ^{125}I-TTR (27% of total radioactivity; *lane 3*). *Error bars*, S.D.

(1.5×10^5) were incubated with E-phyTTR or E-misTTR (0.3 μM) in PBS for 1 h at 4 °C to minimize B cell receptor (BCR) internalization. Competition studies were done by preincubating B cells (1 h, 4 °C) with control diluent or non-biotinylated misTTR, phyTTR, or ovalbumin (3 μM). Bound biotinylated probes were detected with streptavidin conjugated to phycoerythrin-Cy7 (PECy7-SA; 8 μg/ml). IgM$^+$ cells were identified with antibody to human IgM conjugated to FITC (2 μg/ml; BD Pharmingen). Flow cytometry was done using an LSRFortessa X-20 flow cytometer (BD Biosciences) and FlowJo software (about 10,000 cells/analysis). In control incubations, B cells were stained with FITC-labeled, isotype-matched antibody instead of the anti-IgM antibody or were treated with diluent instead of the biotinylated E-misTTR followed by staining with PECy7-SA. The E-misTTR binding cells were visualized by confocal microscopy as described (1) (multiple acquisitions, thickness 0.15 μm; deconvolution by 15 iterations; FITC, λ_{ex} = 488 nm, λ_{em} = 525 nm; 4,6-diamino-2-phenylindole, λ_{ex} = 350 nm, λ_{em} = 470 nm; PECy7, λ_{ex} = 488 nm, λ_{em} = 767 nm).

Amyloid Dissolution—Preaggregated non-radioactive TTR (7.1 μM, 100 μg/ml) was incubated in duplicate with diluent or mIgMs (120 μg/ml) in PBS containing 0.1 mM CHAPS at 37 °C. The dissolution reaction was monitored from turbidity or ThT binding measurements.

Statistical Analysis—Errors are S.D. values. *p* values were from the unpaired two-tailed Student's *t* test. Correlations were determined by Pearson's two-tailed test.

RESULTS

^{125}I-TTR Substrate—Wild type human TTR radiolabeled with ^{125}I (^{125}I-TTR) was applied to determine hydrolysis of the phyTTR tetramers and misTTR aggregates. Non-aggregated ^{125}I-TTR preparations behaved as predicted from studies on phyTTR tetramers (30–32). The non-aggregated ^{125}I-TTR (*a*) did not bind appreciably to ThT (Fig. 1*A*), a probe for β-sheet structures; (*b*) formed minimal particulate aggregates detected by turbidimetry (Fig. 1*B*); and (*c*) dissociated from the 4-mer into the 1-mer state upon boiling in SDS (14 kDa band in Fig.

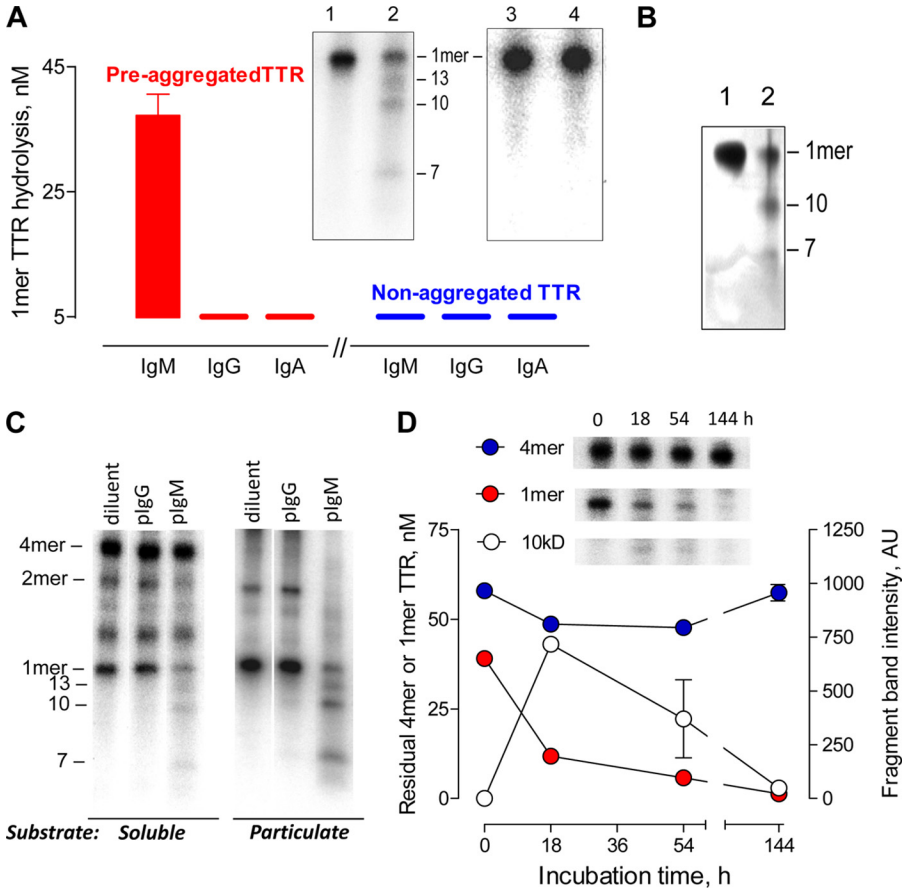

FIGURE 2. **Selective misTTR hydrolysis by polyclonal IgM.** *A*, IgM class-restricted hydrolytic activity. Boiled reaction mixtures of preaggregated or non-aggregated ^{125}I-TTR (*red* and *blue bars*, respectively; 100 nM; misTTR content, 40%) treated for 18 h with diluent or IgM, IgG, and IgA purified from human serum (130 μg/ml, pooled from sera of 12 healthy humans) were electrophoresed. Hydrolysis was determined from depletion of the 1-mer band intensity after antibody treatment relative to the band intensity after diluent treatment. *Inset*, electrophoresis lanes showing depletion of the 1-mer band in preaggregated ^{125}I-TTR treated with IgM (*lane 2*) compared with diluent (*lane 1*). Products are visible as 13, 10, and 7 kDa bands. No 1-mer band depletion or products were evident in the pIgM-treated, non-aggregated ^{125}I-TTR (*lane 4*) compared with the diluent-treated substrate (*lane 3*). *B*, hydrolysis of non-radiolabeled, misTTR by polyclonal IgM. Silver-stained electrophoresis gel of preaggregated TTR (4.5 μM) treated for 52 h with diluent (*lane 1*) or pooled pIgM (*lane 2*; 570 μg/ml). From densitometry, 85% of the 1-mer band derived from misTTR was depleted by pIgM treatment. The 10- and 7-kDa product fragments are observed. The 13-kDa product is not visible because of poor silver stainability. *C*, hydrolysis of soluble and particulate misTTR species by pIgM. The soluble and particulate fractions of preaggregated ^{125}I-TTR (misTTR content, 37 and >95%, respectively) were treated for 18 h with diluent or polyclonal IgM (pIgM) and IgG (pIgG) purified from the same human serum pool (130 μg/ml). Non-boiled reaction mixtures were analyzed. *D*, misTTR selectivity. The 1-mer band (14 kDa) derived from misTTR but not the 4-mer phyTTR band (54 kDa) of preaggregated ^{125}I-TTR (100 nM; misTTR content, 40%) was depleted as a function of time by treatment with pooled pIgM (130 μg/ml). *Inset*, 4-mer, 1-mer, and 10 kDa band cut-outs from electrophoresis gels; non-boiled reaction mixtures. *Error bars*, S.D.

1*C*, *lane 1*; <1% tetramer content) but remained in the 4-mer 54-kDa state in non-boiled SDS solutions (Fig. 1*C*, *lane 2*; <1% 1-mer content). Incubation of ^{125}I-TTR at acid pH generated misTTR aggregates that bound ThT and formed a turbid suspension (Fig. 1, *A* and *B*). Unlike the 4-mer phyTTR state, the misTTR aggregates were dissociated into 1-mers in SDS without prior boiling (Fig. 1*C*, compare *lanes 2* and *4*). The relative 4-mer/1-mer band intensity in non-boiled, preaggregated ^{125}I-TTR, therefore, is an index of the phyTTR/misTTR ratio (misTTR content of six preaggregated ^{125}I-TTR preparations from densitometry, 49 ± 15%). The particulate fraction recovered from a preaggregated ^{125}I-TTR preparation (~50% of total radioactivity; Fig. 1*D*) was composed almost exclusively of misTTR species (>95% 1-mers in Fig. 1*E*, *lane 2*). The 1-mers were also present at low levels in the supernatant (soluble fraction) of preaggregated but not nonaggregated TTR (compare *lane 3*, Fig. 1*E* with *lane 2*, Fig. 1*C*), consistent with the existence of soluble misTTR states (38, 39). Small radioactivity amounts were found at positions corresponding to the TTR dimer (nominal mass 32 kDa) and unidentified impurities in the starting TTR (20 and 26 kDa). ThT fluorescence and turbidity measurements indicated comparable aggregation of ^{125}I-TTR and non-radiolabeled TTR, suggesting unaltered aggregation properties of the radiolabeled protein. The results show that the phyTTR and misTTR states are distinguishable by electrophoresis.

misTTR but Not phyTTR Hydrolysis by Polyclonal IgMs (pIgMs)—We tested the hydrolytic activity of electrophoretically homogeneous polyclonal IgM, IgG, and IgA pooled from the blood of humans without TTR amyloidosis. The pIgMs hydrolyzed preaggregated ^{125}I-TTR, indicated by depletion of the 1-mer TTR band (14 kDa) in SDS-treated, boiled reaction mixtures (Fig. 2*A*). The hydrolytic activity was detected in every individual pIgM preparation from 12 healthy humans (Table 2) but not IgG or IgA from the same humans. Treatment of non-aggregated ^{125}I-TTR with the pIgMs did not deplete the 1-mer band derived from phyTTR in boiled reaction mixtures, indi-

TABLE 2

1-Mer TTR hydrolytic activity of IgMs

IgM preparations with hydrolytic activity >0.1 nM/h/μg were designated "positive." Polyclonal IgMs were from non-aged humans (<35 years). The hydrolytic activities of IgMs from male and female humans were statistically indistinguishable ($n = 9$ and 3, respectively; $p > 0.05$). Monoclonal IgMs were from patients with Waldenström macroglobulinemia.

	No. of IgMs		Hydrolytic activity			
	Tested	Positive	Range	Mean	S.D.	Median
			nM/h/μg IgM			
Polyclonal IgMs	12	12	0.40–1.64	0.93	0.39	0.98
Monoclonal IgMs	16	12	0.16–2.98	1.51	1.07	1.47

cating that the pIgMs do not degrade phyTTR. Depletion of the 1-mer band in boiled reaction mixtures of the preaggregated substrate, therefore, measures misTTR hydrolysis without interference from phyTTR hydrolysis. The pIgMs also degraded preaggregated TTR without the ^{125}I label (Fig. 2*B*), eliminating radioactivity-related experimental artifacts. Selective recognition of soluble and particulate misTTR species by the IgM was confirmed in tests of non-boiled reaction mixtures. phyTTR does not dissociate into 1-mers without boiling, and the 1-mer band is derived exclusively from the misTTR species. The 1-mer band derived from misTTR but not the 4-mer phyTTR band was progressively depleted with increasing duration of pIgM treatment (Fig. 2, *C* and *D*). Product fragments with mass smaller than the 1-mer TTR band were evident (13 and 10 kDa bands, along with the fainter 7 kDa band; Fig. 2*A*). Accumulation of the 10-kDa product in the initial reaction phase and its subsequent disappearance with further pIgM treatment suggested reuse of this misTTR fragment for further digestion cycles (Fig. 2*D*). The appearance of three radioactive products implies hydrolysis of at least two peptide bonds. Because the radioactivity from a single intact TTR molecule is distributed into multiple products, the product bands are less intense than the intact TTR band. The assay method does not detect small products that migrate out of the gel or products that lack a radiolabeled Tyr residue.

Formation of IgM-misTTR immune complexes by the pooled pIgM (130 μg/ml) was undetectable (binding of soluble and particulate misTTR species, respectively: 1.9 ± 2.4 and 0.7 ± 0.7%). At an equivalent concentration, the same pIgM preparation hydrolyzed 45 ± 1% of soluble misTTR and 77 ± 1% of particulate misTTR, respectively. The results indicate hydrolysis of misTTR but not phyTTR by IgMs, the first class of antibodies produced by B cells. In contrast, the IgGs and IgAs usually associated with acquired immune responses were devoid of misTTR hydrolytic activity.

Polyclonal IgM Hydrolytic Properties—Mean misTTR hydrolysis by pIgM preparations from humans >70 years in age was only slightly lower than the level from humans <35 years in age, and the difference did not reach statistical significance ($p = 0.101$; Fig. 3*A*). misTTR hydrolysis was detected at low pIgM concentrations (10 μg of IgM/ml, ~200-fold lower than the blood IgM concentration). The pIgM hydrolytic rate was comparable with MMP9 (Fig. 3*B*), an enzyme suggested to limit tissue deposition of TTR amyloid (36). The blood IgM concentration, however, exceeds that of MMP9 (3.2 nM) and other non-IgM proteases (<1 nM) by about 3 log orders (40, 41). misTTR is generated from wild type phyTTR slowly at physiological pH (42), and saturation of the IgM by trace misTTR amounts in blood (16) is unlikely. From the observed rates, 50% degradation of 1 nM misTTR at the blood IgM and MMP9 concentrations is predicted to occur in 24 min and 28 days, respectively. Additional findings supported an important role of the IgM: (*a*) the hydrolytic activity of unfractionated human serum was lost nearly completely upon antibody removal by immunoadsorption (Fig. 3*C*); (*b*) the TTR product fragment profiles for purified pIgMs and unfractionated serum were identical (13, 10, and 7 kDa bands; Fig. 3*C*, *inset*); and (*c*) only the 900-kDa pIgM fraction separated from other serum components by FPLC gel filtration expressed hydrolytic activity (Fig. 3*D*).

pIgM-catalyzed misTTR hydrolysis was inhibited by synthetic electrophilic phosphonate **1**, a compound that binds covalently to the nucleophilic sites of serine proteases (Fig. 3*E*). Synthetic inhibitors of metalloproteases, acid proteases, and cysteine proteases were ineffective. The inhibitor profile is consistent with previous findings that catabodies use a nucleophilic proteolytic mechanism (1, 43). Non-antibody proteases are sensitive to endogenous enzyme inhibitors present in serum, and the enzymatic reaction may also be inhibited by amyloid binding proteins (*e.g.* SAP) (36). Including antibody-free human serum or purified SAP in the reaction mixtures did not reduce the misTTR hydrolytic activity of pIgM (compare with control albumin treatment; Fig. 3*E*). Moreover, because misTTR was hydrolyzed by unfractionated IgMs without removal of any serum components, the IgMs are insensitive to serum protease inhibitors. We cannot exclude the possibility of a serum cofactor that enhances IgM catalysis, because the hydrolytic activity of unfractionated serum per unit IgM mass exceeded that of pure pIgM from the same serum by 4.5-fold (7.2 and 1.6 nM/μg of IgM/h, respectively; this is a valid comparison because nearly all of the serum hydrolytic activity is due to the IgMs). Catabody-activating cofactors were described previously (44, 45). Alternatively, because catabodies are sensitive to conformational perturbations (29), the acid elution procedure employed for IgM purification may attenuate the hydrolytic activity.

The pIgM hydrolytic activity was saturable with increasing misTTR concentration (Table 3). In addition to misTTR, the pIgMs hydrolyzed small peptide substrates, a reaction that reports the catalytic subsite properties independent of noncovalent epitope binding (1, 46). The apparent K_m for misTTR was 92-fold lower than that of EAR-AMC, a small peptide hydrolyzed by IgMs at the Arg-AMC bond, suggesting selective IgM-misTTR recognition (K_m approximates K_d, the equilibrium dissociation constant). Diffusional restrictions known to decelerate enzymatic conversion of particulate substrates compared with soluble substrates (47, 48) probably limit the rate of particulate misTTR hydrolysis by the IgMs. The pIgM preparations are mixtures of individual IgM subsets, and misTTR is a mixture of multiple misTTR aggregation states. The apparent kinetic constants, therefore, are average values for hydrolysis of multiple misTTR species by multiple IgMs.

misTTR-directed B Cells and mIgMs—The reactivity of mIgMs expressed as BCRs in healthy humans often indicates initial antibody specificity prior to contact with external

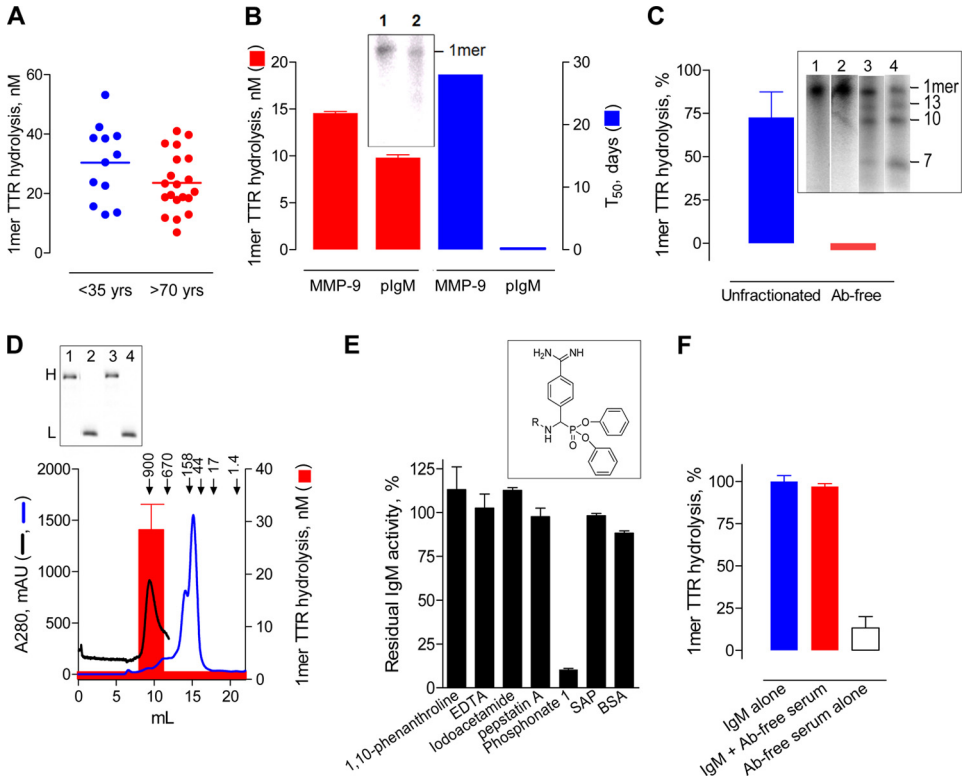

FIGURE 3. **Characterization of polyclonal IgM hydrolytic activity.** *A*, comparison of hydrolytic activity of individual pIgM preparations (90 μg/ml) from non-aged (<35 years, $n = 12$) and aged humans (>70 years, $n = 20$) determined by electrophoresis. Shown are the hydrolysis levels estimated using the preaggregated ^{125}I-TTR substrate (160 nM; misTTR content, 60%; 18-h incubation) and non-boiled reaction mixtures. *B*, rates of preaggregated ^{125}I-TTR hydrolysis by MMP9 and pIgM (*left axis*). MMP9 and pIgM concentrations were 133 nM. Other conditions were as in *A*. T_{50} (*right axis*) is the time required to hydrolyze 50% of 1 nM misTTR at the MMP9 or pIgM concentrations in blood (3.2 nM and 2.2 μM, respectively, computed from the equation, $S = S_0(1 - e^{-[Eo]kt})$, where S_0 is substrate concentration at time 0, E_0 is the enzyme concentration at time 0, k is the second order rate constant derived from the equilibrium binding and catalytic constants, and t is reaction time. *Inset*, SDS gel showing reduced 1-mer misTTR band following MMP9 treatment (*lane 2*) compared with diluent treatment (*lane 1*). *C*, pIgM immunoadsorption. misTTR hydrolysis by unfractionated human serum and Ab-free serum was measured as in *A*. The protein content of unfractionated serum (diluted 1:100) and the antibody-free serum was adjusted to be identical (1.14 mg/ml). IgM concentrations in hydrolysis assays using unfractionated serum and antibody-free serum were 20 and <0.01 μg/ml, respectively. Data are expressed as percentage depletion of the 1-mer misTTR band compared with the control substrate reaction mixture treated with diluent (100% value = 22.5 ± 5.6 nM). *Inset*, electrophoresis showed identical product fragments (13, 10, and 7 kDa bands) generated by digesting preaggregated ^{125}I-TTR with unfractionated serum (*lane 3*, 1:100 dilution) and purified IgM (*lane 4*, 120 μg/ml). *Lane 1*, substrate treated with diluent. *Lane 2*, substrate treated with antibody-free serum. *D*, distribution of hydrolytic activity of unfractionated serum. Only the IgM-containing 900-kDa fraction (retention volume 8–11 ml) obtained by FPLC gel filtration of human serum (*blue trace*) displayed detectable misTTR hydrolytic activity assayed as in *A* (*red bars*). IgM concentration in the assay, 20 μg/ml (equivalent to IgM concentration in 1% unfractionated serum). Elution of reference purified IgM (*black trace*) is coincident with elution of the serum hydrolytic activity. Non-IgM serum fractions were tested as two pools at a concentration corresponding to 1% unfractionated serum equivalents (retention volume 0–8.0 and 11.0–22.0 ml; concentrated using a 3-kDa ultrafilter). *Inset*, reducing SDS gels of 900-kDa serum IgM fraction showing anti-μ antibody-stained 70-kDa heavy chain band (*lane 1*) and anti-λ/κ antibody-stained 25-kDa light chain band (*lane 2*). *Lanes 3* and *4*, respectively, are similarly stained heavy and light chain bands of the reference IgM, respectively. *H*, heavy chain; *L*, light chain. *E*, protease inhibitor effects. misTTR hydrolysis was measured using IgM pretreated (1 h) with diluent or the indicated inhibitors of metalloproteases, cysteine proteases, acid proteases, and serine proteases. The structure of phosphonate **1** is shown. SAP is an amyloid-binding protein. Residual hydrolytic activity of inhibitor-treated IgMs was computed as a percentage of IgM activity after treatment with diluent (100% value = 24 ± 4 nM TTR). Hydrolysis was measured using boiled reaction mixtures of 100 nM preaggregated ^{125}I-TTR incubated with 60 μg IgM/ml for 18 h. *F*, unimpeded hydrolysis of preaggregated ^{125}I-TTR by pIgM in the presence of Ab-free serum. Plotted are 1-mer misTTR hydrolytic activities expressed as a percentage of the activity of purified (130 μg/ml) alone (90 ± 3 nM). Reaction conditions were as in *A*. *Error bars*, S.D.

TABLE 3

Apparent kinetic parameters for hydrolysis of preaggregated TTR by polyclonal IgM

K_m is reported as μM substrate. V_{max} is reported as μM substrate hydrolyzed over 5 days (IgM half-life in blood) at the IgM concentration in blood (2 mg/ml). Values are from hydrolytic rates at increasing concentrations of preaggregated ^{125}I-TTR fitted to the Michaelis-Menten equation (160 nM to 14.4 μM, misTTR content 60%; r^2 = 0.94); IgM, 70 μg/ml.

Substrate	K_m	V_{max}
Preaggregated TTR	1.3 ± 0.3	269.3 ± 15.8
EAR-AMC	120 ± 11	44,352 ± 1,584

immunogens. The E-misTTR analog contains electrophilic phosphonates that bind covalently to nucleophilic BCR sites responsible for catalysis, permitting identification of misTTR-selective B cells without loss of the bound probe due to peptide-bound hydrolysis. Flow cytometry identified a discrete IgM$^+$ B cell population with saturable binding activity for E-misTTR that was inhibited by competitor misTTR but not the irrelevant protein ovalbumin (Fig. 4*A*). The intensity of E-misTTR staining differed over 2 log orders, suggesting the variable E-misTTR reactivity of individual B cells. Saturable E-phyTTR binding by the B cells was negligible, indicating selective recognition of the E-misTTR probe (Fig. 4*B*). Most of the E-misTTR binding sites were colocalized with cell surface IgM, consistent with BCR recognition of the misTTR (Fig. 4*C*, *image 3* is a merged rendition).

A panel of mIgMs secreted by cancerous B cells from patients with Waldenström macroglobulinemia without TTR amyloidosis was applied as a model for individual IgMs present in

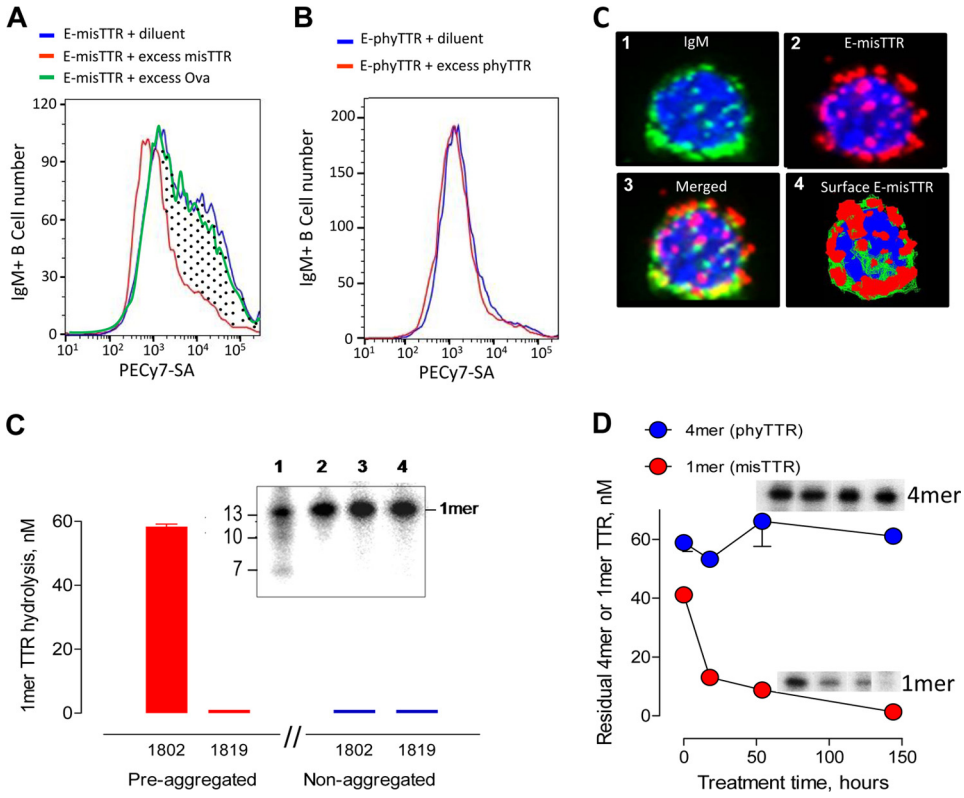

FIGURE 4. **Selective misTTR recognition by B cells and monoclonal IgMs.** *A*, selective E-misTTR binding by human IgM$^+$ B cells. Profile of PECy7-SA-stained IgM$^+$ B cells treated with E-misTTR in diluent or excess non-biotinylated misTTR. The *dotted area* represents IgM$^+$ B cells with saturable E-misTTR binding activity (45% of total IgM$^+$ B cells). E-misTTR binding was not affected in the presence of excess ovalbumin (*Ova*). *B*, nearly equivalent binding of the cells to E-phyTTR was evident in diluent and in the presence of excess phyTTR, suggesting the absence of saturable E-phyTTR reactivity. *C*, E-misTTR binding to IgM$^+$ B cells. Deconvoluted images show an IgM$^+$ B cell stained with FITC-conjugated antibody to IgM (*image 1*, *green*), the cell stained with PECy7-SA to visualize E-misTTR binding (*image 2*, *red*), the merged rendition (*image 3*), and the reconstituted three-dimensional model suggesting E-misTTR binding to cell surface BCRs (*image 4*). *Blue counterstain*, 4′,6-diamidino-2-phenylindole; magnification, ×60. *D*, misTTR hydrolysis by monoclonal IgM 1802. The reaction mixtures of preaggregated or non-aggregated ^{125}I-TTR (100 nM) treated with diluent or hydrolytic mIgM 1802 (18 h, 60 μg/ml) were boiled, thereby dissociating both phyTTR and misTTR into 1-mers (14 kDa). IgM 1819 is one of four IgMs devoid of misTTR hydrolytic activity. *Inset*, electrophoresis gel showing preaggregated ^{125}I-TTR treated with IgM 1802 (*lane 1*) or mIgM 1819 (*lane 2*) and non-aggregated ^{125}I-TTR treated with mIgM 1802 (*lane 3*) or mIgM 1819 (*lane 4*). Product profiles were similar to the polyclonal IgM digests. *E*, time-dependent misTTR hydrolysis. mIgM 1802 treatment (120 μg/ml) depleted the 1-mer band derived from misTTR but not the 4-mer phyTTR band visualized by electrophoresis (assay conditions as in *A*). *Insets*, electrophoresis gel cut-outs of the 4-mer phyTTR band and 1-mer misTTR band at the four time points tested (*left* to *right*: 0, 18, 54, and 154 h). *Error bars*, S.D.

the pIgM preparations.[3] Twelve of 16 mIgMs hydrolyzed preaggregated ^{125}I-TTR (Table 2). The hydrolytic rates were highly variable (undetectable to 2.98 nM/μg of IgM/h), consistent with the prediction of differing catalysis by individual catabodies with structurally distinct V domains. Like the pIgMs, the 12 misTTR-hydrolyzing mIgMs hydrolyzed misTTR but not phyTTR, shown by (*a*) the depleted 1-mer band of preaggregated ^{125}I-TTR but not non-aggregated ^{125}I-TTR in boiled reaction mixtures and (*b*) the depleted 1-mer TTR band originating from misTTR and the undepleted 4-mer phyTTR band in non-boiled reaction mixtures of pre-aggregated ^{125}I-TTR (Fig. 4, *D* and *E*, shows the example of mIgM 1802). Moreover, the mIgMs generated the same 13-, 10-, and 7-kDa TTR product fragments observed for pIgMs (Fig. 4*C*, *inset*). The consistent selectivity and product fragment profiles suggest a shared structural basis for mIgM and pIgM catalysis.

From mutagenesis (43), epitope mapping (49), and protease inhibitor studies (50), we proposed the split site catalysis model (Fig. 5*A*), involving discrimination between structurally distinct antigen epitopes by the noncovalent binding site prior to peptide bond hydrolysis at the catalytic subsite. At saturating concentrations, the short peptide EAR-AMC substrate is hydrolyzed detectably by the catalytic subsite, a test for catalysis occurring without selective epitope recognition (1, 46). As reported (7), titration of mIgM Yvo with the phosphonate **1** inhibitor indicated 10.2 EAR-AMC hydrolytic sites/IgM molecule (Fig. 5*B*, *inset*; theoretical number of catalytic sites/IgM, 10). When tested as an alternate substrate, EAR-AMC inhibited the misTTR hydrolytic activity of mIgM Yvo (Fig. 5*B*). Ala-Ala-Ala-AMC (AAA-AMC), a peptide that is not hydrolyzed by the mIgM, did not inhibit the misTTR hydrolytic activity. It may be concluded that misTTR and EAR-AMC hydrolysis occur at the same mIgM catalytic site. In addition, EAR-AMC and misTTR hydrolysis by the panel of 16 mIgMs was significantly correlated ($p = 0.005$; Fig. 5*C*), consistent with regulation of misTTR

[3] The panel is assumed to be a random collection of mIgMs. There is no known relationship between B cell carcinogenicity and IgM catalytic activity or antigenic specificity. Studies to be published elsewhere confirmed secretion of monoclonal IgMs by Epstein-Barr virus-transformed B cells from healthy humans with misTTR-hydrolyzing activity in a range similar to IgMs from Waldenström macroglobulinemia patients (S. A. Planque, S. K. Murphy, S. Sonoda, E. L. Brown, and S. Paul, manuscript in preparation).

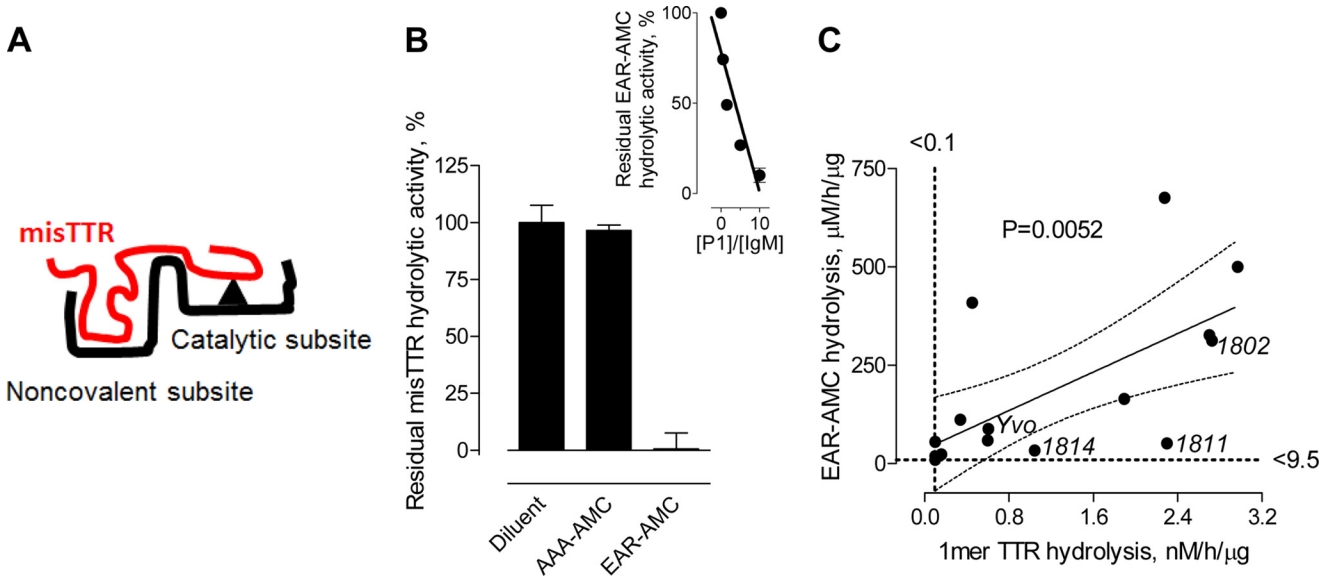

FIGURE 5. **Relationship between EAR-AMC and misTTR hydrolysis by monoclonal IgMs.** *A*, split site catabody model. Catabody selectivity derives from initial epitope recognition by the noncovalently binding subsite followed by peptide bond hydrolysis at a spatially proximate catalytic subsite. Small peptide substrates are hydrolyzed at the catalytic subsite without dependence on the noncovalent binding subsite. *B*, misTTR and EAR-AMC hydrolysis at a shared catalytic subsite. Hydrolysis of preaggregated ^{125}I-TTR (100 nM; misTTR content, 40%) by mIgM Yvo (300 μg/ml) was measured in the presence of the alternate substrates EAR-AMC or AAA-AMC (1 mM; incubation for 18 h). IgM hydrolytic activity is expressed as a percentage of activity in diluent instead of alternate substrate (45 $\pm$ 3 nM). *Inset*, data from Ref. 7 showing stoichiometric inhibition of mIgM Yvo-catalyzed EAR-AMC hydrolysis at varying phosphonate **1**/IgM molar ratios. The *x* intercept is the number of catalytic sites/mIgM molecule. *C*, correlated EAR-AMC and misTTR hydrolysis by mIgMs. EAR-AMC hydrolysis by the panel of 16 mIgMs was measured fluorimetrically (1). misTTR hydrolysis was measured as in Fig. 4 using boiled reaction mixtures. *Solid* and *dotted lines* show the least-square regression fit (Pearson $r^2 = 0.44$, $p < 0.005$) and 95% confidence band, respectively. *Error bars*, S.D.

hydrolysis by the catalytic subsite efficiency. Importantly, the concentration of misTTR required for detection of hydrolysis was ~3 log orders lower than the EAR-AMC substrate, consistent with selective misTTR recognition. Certain mIgMs with low EAR-AMC hydrolytic activity hydrolyzed misTTR robustly (*e.g.* IgMs 1811 and 1814 falling outside the regression confidence limits in Fig. 5*C*), suggesting that hydrolysis can be accelerated due to selective misTTR recognition.

Are the Catabodies Polyreactive?—The complementarity-determining regions (CDRs) of some polyreactive IgMs produced without immunogen stimulation can bind epitopes with no discernible structural similarity (51), a phenomenon that may originate from CDR flexibility and the induced fit binding mechanism. Consistent with previous reports (2, 7), the pIgMs and mIgMs did not hydrolyze non-amyloidogenic, non-superantigen proteins from eukaryotic and prokaryotic organisms (Fig. 6*A*; no hydrolysis of albumin, extracellular epidermal growth factor receptor fragment, ovalbumin, transferrin, collagen adhesion protein, or LukS). Specific catalysis requires spatial coordination between the catabody noncovalent and catalytic subsites (2). The lack of indiscriminate pIgM proteolysis may be explained by uncoordinated CDR-based, polyreactive binding activity and catalytic subsite activity.

The misTTR-hydrolyzing mIgM Yvo was reported to hydrolyze Aβ40 and Aβ42 peptides (7), a reactivity pattern reminiscent of antibodies that bind the β-strand conformational epitope of amyloids without dependence on the epitope sequence (52, 53). In contrast, the misTTR hydrolyzing mIgM 1802 did not hydrolyze preaggregated Aβ42 (Fig. 6*B*), suggesting sequence-selective misTTR recognition. Only 2 of 9 misTTR-hydrolyzing mIgMs tested hydrolyzed Aβ40 (Fig. 6*C*). Certain misTTR-hydrolyzing mIgMs also hydrolyzed HIV protein gp120, a B cell superantigen (2). Superantigens are recognized noncovalently at the framework regions of reversibly binding antibodies (54–56) and catabodies (57, 58), and the framework regions also play a direct role in peptide bond hydrolysis (43). We studied the correlations between hydrolysis of misTTR, gp120, and another superantigenic protein, *S. aureus* Protein A (56). A minority of misTTR-hydrolyzing mIgMs hydrolyzed Protein A (3 of 16 IgMs; Fig. 6*D*) and a majority hydrolyzed gp120 (13 of 16; Fig. 6*E*). There was no correlation between misTTR and gp120 or Protein A hydrolysis ($p > 0.05$). Two misTTR-hydrolyzing mIgMs did not hydrolyze Aβ, Protein A, or gp120 (IgM 1802 and 1814). mIgM Yvo was the only catabody with hydrolytic activity directed to all four amyloid/superantigen substrates (misTTR, Aβ, Protein A, and gp120). misTTR hydrolysis by this mIgM was inhibited by the alternate substrate Aβ but not gp120 or Protein A (Fig. 6*F*), suggesting that occupancy of the superantigen-interacting sites does not impede misTTR hydrolysis. The studies indicated variable mIgM reactivity profiles, including mIgMs monoreactive for TTR and mIgMs with amyloid/superantigen-directed oligoreactivity.

misTTR Dissolution—Treatment of a 10-fold molar excess of preaggregated TTR with the hydrolytic mIgM 1802 but not non-hydrolytic IgM 1819 resulted in time-dependent reduction of turbidity to the nearly basal value of non-aggregated TTR (Fig. 7*A*). ThT binding by preaggregated TTR, an indicator of β-sheet content, was also reduced to the nearly basal value by the hydrolytic but not the non-hydrolytic mIgM (Fig. 7*B*). The observed dissolution rate is diffusion-restricted by the particulate substrate character, and the dissolution process probably proceeds through a series of hydrolytic reactions, eventually converting particulate misTTR to soluble products. The

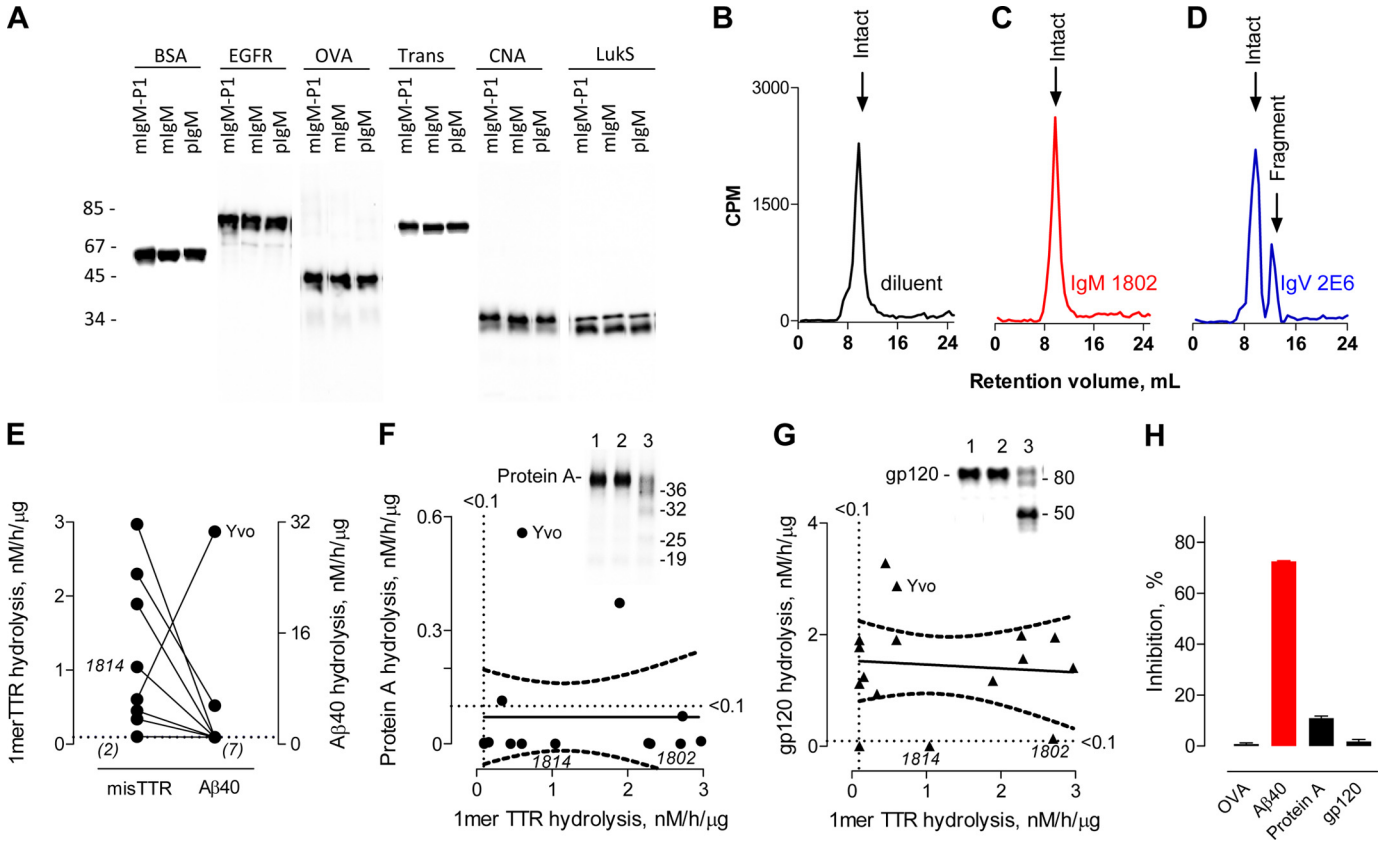

FIGURE 6. **Monoreactive and oligoreactive misTTR hydrolyzing monoclonal IgMs.** *A*, no hydrolysis of non-amyloid and non-superantigen proteins. Shown are SDS electrophoresis gels containing reaction mixtures of the following biotinylated proteins treated for 22 h with pIgM (pooled from 12 humans) or mIgM 1802 (130 μg/ml): extracellular domain of epidermal growth factor receptor (*exEGFR*), bovine serum albumin (*BSA*), ovalbumin (*OVA*), transferrin (*Trans*), and two *S. aureus* virulence factors, LukS and collagen adhesion protein CNA. *mIgM-P1*, control reaction mixture containing IgM 1802 inhibited by electrophilic phosphonate **1**. *B–D*, no fibrillar Aβ hydrolysis by mIgM 1802. FPLC gel filtration profiles of formic acid-solubilized reaction mixtures containing fibrillar ^{125}I-Aβ42 (30,000 cpm) treated for 16 h with diluent (*B*), monoclonal mIgM 1802 (120 μg/ml) (*C*), or the Aβ-hydrolyzing immunoglobulin V domain fragment (IgV 2E6, 10 μg/ml) (*D*). No depletion of intact ^{125}I-Aβ42 (computed mass 4,630 Da) or product appearance was evident by mIgM treatment, whereas IgV 2E6 generated a radioactive fragment with a mass of 1654 Da corresponding to hydrolysis at the His^{14}–Gln^{15} bond (29). *E*, discordant misTTR and Aβ hydrolytic activities of mIgMs ($n = 9$). Aβ40 hydrolysis data are from Ref. 7. *Connecting lines* identify individual mIgMs. In *parentheses* are the number of mIgMs without detectable activity. misTTR-monoreactive mIgM 1814 and oligoreactive mIgM Yvo are identified. *F*, discordant misTTR and Protein A hydrolytic activities of mIgMs ($n = 16$). Hydrolysis of biotinylated Protein A (72 nM) following IgM treatment (45 μg/ml, 72 h) was determined electrophoretically. *Solid* and *dotted lines*, least-square regression fit and 95% confidence bands, respectively ($p > 0.05$, $r^2 < 0.001$; two-tailed Pearson analysis). misTTR-monoreactive mIgMs 1802 and 1814 and oligoreactive mIgM Yvo are identified. *Inset*, SDS-gel electrophoresis lanes of Protein A treated with diluent (*lane 1*), non-hydrolytic mIgM 1801 (*lane 2*), and hydrolytic mIgM Yvo showing depletion of intact Protein A and the appearance of smaller mass products (*lane 3*). *G*, hydrolysis of biotinylated gp120 (100 nM) following IgM treatment (45 μg/ml, 18 h) was determined electrophoretically. *Solid* and *dotted lines* are the least-square regression fit and 95% confidence bands, respectively ($p > 0.05$, Pearson $r^2 = 0.007$). misTTR-monoreactive mIgMs 1802 and 1814 and oligoreactive mIgM Yvo are identified. *Inset*, SDS-gel electrophoresis of gp120 treated with diluent (*lane 1*), non-hydrolytic mIgM 1801 (*lane 2*), and hydrolytic mIgM Yvo showing depletion of intact gp120 and appearance of smaller mass product bands (*lane 3*). *H*, inhibition of mIgM Yvo catalyzed misTTR hydrolysis by alternate substrates. Only Aβ inhibited the misTTR hydrolytic activity. Like the irrelevant protein ovalbumin (*OVA*), the superantigens Protein A and gp120 were non-inhibitory. Concentration of alternate substrates was 1 μM, and that of mIgM Yvo was 130 μg/ml. Other reaction conditions were as in Fig. 4*A*. *Error bars*, S.D.

mIgMs (130 μg/ml) did not form detectable immune complexes (percentage of soluble and particulate ^{125}I-misTTR binding: hydrolytic mIgM 1802, 1.9 ± 1.6 and 0.3 ± 0.1%, respectively; non-hydrolytic mIgM 1819, 1.0 ± 2.6 and 1.6 ± 1.6%, respectively). Because the hydrolytic mIgM 1802 has no misTTR binding activity and, except for the V domains, is structurally identical to the non-hydrolytic mIgM, the dissolution reaction must be due to misTTR digestion.

DISCUSSION

Small misTTR amounts are probably produced as normal byproducts of alternate TTR folding pathways. With advancing age, such misTTR species are thought to serve as seeds for pathological TTR amyloid formation. Our findings suggest physiological production of misTTR-selective IgM catabodies as a first line defense function against TTR amyloidosis. The IgMs hydrolyzed soluble and particulate misTTR but not the non-pathogenic phyTTR tetramer found at micromolar concentrations in blood, suggesting selectivity for an aggregation-induced misTTR neoepitope that is absent in phyTTR. The IgMs, therefore, can degrade misTTR with no danger of saturation by the more abundant phyTTR species. There was no evidence for IgM degradation of non-amyloid, non-superantigen proteins (2, 7). Two misTTR-hydrolyzing mIgMs did not hydrolyze Aβ or microbial superantigens, and other mIgMs recognized these substrates at varying levels. Saturation of oligoreactive IgMs with irrelevant amyloids may limit the misTTR clearance capacity, but this is a threat only in patients with non-TTR amyloid disease. Likewise, superantigens accumulate only during microbial infections, and impairment of misTTR clearance

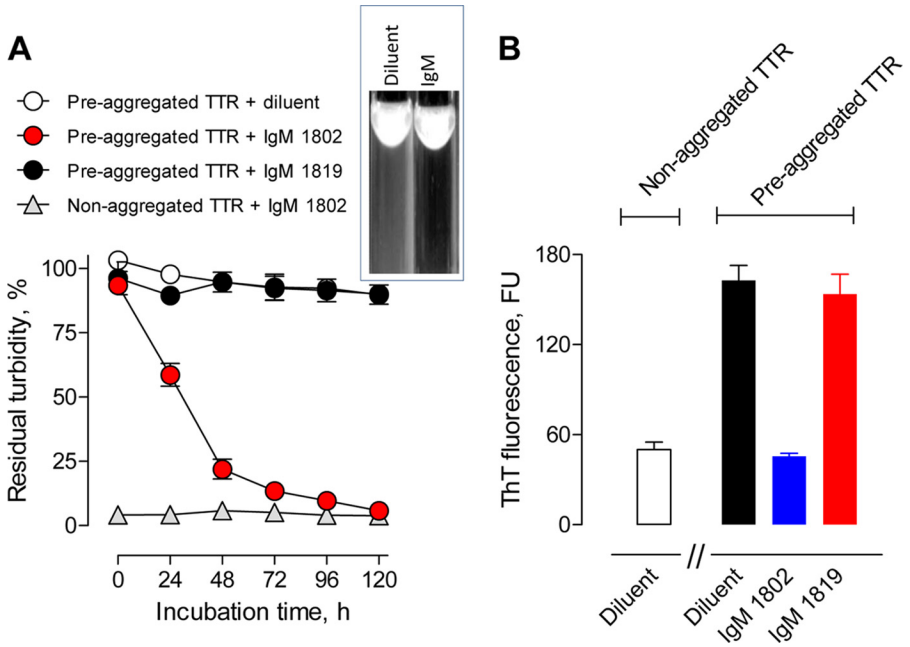

FIGURE 7. **Dissolution of preaggregated TTR by mIgM 1802.** *A*, reduced turbidity. Preaggregated TTR (7.1 μM) was incubated in the presence of hydrolytic mIgM 1802 (120 μg/ml, 0.67 μM), an equivalent non-hydrolytic IgM 1819 concentration, or diluent. mIgM 1802 treatment reduced the turbidity to the basal value observed for control non-aggregated TTR treated with mIgM 1802. *Inset*, photograph showing turbid misTTR suspension (*white precipitates* against *black background*) following incubation in diluent and misTTR dissolution after treatment with the hydrolytic IgM. *B*, reduced ThT fluorescence. Shown are ThT fluorescence values after treating preaggregated TTR with hydrolytic mIgM 1802, non-hydrolytic mIgM, or diluent for 120 h as in *A*. mIgM 1802 treatment reduced the ThT fluorescence value to the basal value observed for non-aggregated TTR treated with diluent. Data are corrected for ThT fluorescence of IgMs alone without TTR substrate (84 ± 5 fluorescence units (*FU*)). *Error bars*, S.D.

is not predicted in the non-infected state. The selectivity properties, therefore, support a role for the IgMs in defense against TTR amyloidosis.

Further evidence for the beneficial IgM role includes the following: (*a*) preaggregated TTR was dissolved completely by a hydrolytic mIgM; (*b*) misTTR was degraded at IgM concentrations ~200-fold lower than the blood IgM concentration, and virtually the entire misTTR degradative capacity of serum was attributable to IgMs; (*c*) the blood IgM concentration exceeds that of non-antibody proteases by several log orders, and pIgMs hydrolyzed misTTR at a rate comparable with that of a non-antibody protease (MMP9); (*d*) the pIgM hydrolytic activity was refractory to serum inhibitors of non-antibody proteases; and (*e*) pIgM from different healthy adults hydrolyzed misTTR within a narrow rate range, suggesting stable maintenance of the misTTR hydrolytic activity under disease-free conditions. The beneficial IgM function may extend beyond clearance of blood-borne misTTR. IgMs permeate most anatomic blood-tissue barriers. Lymph from many tissues, a common surrogate for the tissue interstitial fluid, contains IgM in the mg/ml range (59–61), indicating the feasibility of tissue misTTR clearance.

Notwithstanding the favorable catabody properties, pathological TTR amyloid accumulates in SSA patients, indicating that the catabody clearance capacity may be overwhelmed by independent age-associated factors that accelerate protein misfolding (*e.g.* the reaction of amyloidogenic proteins with advanced glycation and lipid peroxidation end products) (62, 63). In addition, we cannot exclude reduced catabody formation as a possible factor in TTR amyloidosis. Age-associated shifts in the structural and functional properties of antibody V domains are documented (64, 65), individual mIgMs hydrolyzed misTTR at widely variable rates, and aged humans display increased susceptibility to infections (66). We observed a small, non-significant tendency toward reduced misTTR hydrolysis in healthy, aged humans. Future studies on patients with SSA are required to assess whether immune senescence is a predisposing factor in amyloidosis. In addition, long term follow-up of humans and mice with genetic antibody deficiencies (67, 68) may be useful to define the contribution of the immune system in defense against amyloidosis. The catalytic function may also be conceived to diminish the inflammatory consequences of antibody-antigen interactions. Reversible binding at the Fab region of conventional antibodies stimulates Fc region-mediated activation of complement and phagocytosis, exemplified by the inflammatory effects of Aβ-binding antibodies (69). Rapid catabodies form only transient immune complexes and then release the digested antigen products, reducing the probability of harmful immune complex effects.

According to the acquired immunity paradigm, IgGs with specific binding activity directed to individual target epitopes are produced within a few weeks by the immunogen-driven maturation of antibody light and heavy chain variable domain sequences (V_L and V_H domains, respectively). Acquired immunity rules did not yield catabodies capable of complex peptide bond hydrolytic reactions (70). Moreover, the rules provide no basis to anticipate the strict catabody selectivity for misTTR. Because misTTR-directed IgMs are produced by healthy humans without TTR amyloidosis, they are probably produced constitutively without a requirement for acquired immunity processes. Catabody synthesis can occur without immunogen-driven V domain maturation because the serine protease-like nucleophilic sites are encoded by heritable germ line V region

genes (3–6). A germ line V_L gene residue is an essential constituent of the misTTR-hydrolyzing mIgM Yvo catalytic triad (Ser^{110}, IMGT numbering), and the two remaining catalytic residues are evidently acquired during V-(D)-J gene recombination, which occurs prior to contact with the immunogen (Arg^{112} and Glu^{113} at the V_L-J and V_HD-J junctions, respectively (71)). Furthermore, the IgMs are the first antibody class produced by B cells, whereas IgGs generated at the terminal acquired immunity stage are poorly hydrolytic. The antibody C domain scaffold can influence antigen binding at the remote V domains (72). C domain swapping studies indicated loss of catalytic activity at the IgM → IgG class switch step due to the unfavorable effect of the IgG C domains on the V domain catalytic site (28). Detailed information about factors regulating IgM constitutive synthesis is not available. However, IgMs are synthesized at stable levels by germ-free animals (73), and their constitutive production may involve an autonomous B cell developmental program and BCR-independent lymphocyte growth stimulators (74).

In adult humans, IgGs are the dominant blood-borne antibodies, found at 5–6-fold greater concentrations than IgMs. Many IgGs express specific antigen binding activity, consistent with maturation of their V domains by an immunogen-driven somatic mutation process. Such antigen-specific IgGs are the basis of protective responses induced by microbes and vaccines, and numerous antigen-binding monoclonal IgGs are approved for therapeutic use (75). Catalytic IgG preparations from patients with autoimmune disease are reported to hydrolyze self-antigens (8, 76–78), but dysfunctional B cell reactivity in autoimmune disease may contribute to increased catalytic IgG synthesis (8), and the hydrolytic rate of the IgGs is usually lower than that of IgMs (79, 80). Monoclonal IgGs from routine immunization protocols display minimal or no catalytic activity, but their dissociated light subunit frequently hydrolyzes peptide bonds (81–83). Other IgGs generated by healthy humans express low affinity, polyreactive antigen binding profiles (often designated "natural" IgGs) that may originate from the occurrence of class switch recombination in bystander B cells without sufficient mutations in the V domains required to accomplish specific antigen binding (84, 85). The polyreactivity was suggested to contribute in the therapeutic effect of pooled IgGs from healthy humans in patients with bacterial infections and certain autoimmune diseases (commonly known as intravenous immune globulin or IVIG preparations) (86). The catalytic activity of such IVIG preparations is marginal compared with IgMs (27). Also, the IgMs in the present study display catalytic specificities that are readily distinguishable from the polyreactive IgG binding pattern.

Protein-protein recognition is dictated by sequence-dependent chemical interactions, topographical shape complementarity, and local flexibility of the reacting sites. The amyloid-superantigen link is obvious from mIgMs with oligoreactivity for both protein classes (*e.g.* mIgM Yvo). Comparison of linear sequences did not indicate a homologous epitope that is shared by TTR, Aβ, Protein A, and gp120 (Fig. 8*A*). Our innate catabody model conceives an initial selectivity-conferring binding step that places the substrate peptide backbone in spatial register with the catabody hydrolytic subsite (8, 43). The oligoreactivity may originate from substrate interactions at a single cross-reactive catabody site or multiple catabody sites with unique ligand preferences. Antibody V domains are described to express multiple ligand-interacting sites outside the classical CDR-based antigen binding pocket (87). For instance, the framework region-based V_H domain sites that recognize Protein A and gp120 are not identical (54, 55), and yet another V_L domain site recognizes the superantigen Protein L (88). Because misTTR hydrolysis by mIgM Yvo was not inhibited competitively by Protein A and gp120, non-identical sites are probably involved in hydrolysis of misTTR *versus* superantigens. In contrast, Aβ inhibited the hydrolysis of misTTR, suggesting amyloid substrate recognition at a shared IgM site. A precedent for the TTR/Aβ cross-reactive site is available; reversibly binding antibodies can recognize the β-strand conformational epitope found in amyloid proteins with differing sequence (52, 53).

Humans produce no more than 100,000 non-antibody proteins, including all known enzymes and receptors with specificity for a broad range of ligands. The recombined IgM repertoire derived from the germ line V, D, and J segment configurations is far larger (from germ line gene sequences available in IgBLAST, $\sim 4 \times 10^9$ V_L-V_H domain pairs derived by recombination of 152 V_L with 19 J genes and recombination of 273 V_H genes with 34 D and 13 J genes; this estimate excludes further repertoire expansion occurring during the junctional diversification process). We suggest the human germ line IgM repertoire as a source of catabodies with functionally useful selectivity for individual substrates developed by Darwinian immune evolution (Fig. 8*B*). Like the misTTR-selective catabodies, the innate character of catabodies to Aβ is evident from superior Aβ hydrolysis by IgMs compared with IgGs and by production of Aβ binding and hydrolyzing antibodies by healthy humans without amyloidosis (7, 89). Jawed fish, the first extant organisms with an immune system orthologous to humans, produce TTR and Aβ with sequences similar to their human counterparts (Fig. 8*C*). Because tissue amyloid deposition has no known benefit in eukaryotes, the catabodies may have evolved to retard amyloidosis. Amyloids of 27 proteins can accumulate to pathogenic levels, causing premature senescence and disease (11). Proteins accumulate in the amyloid state within minutes to days *in vitro*, suggesting the existence of functionally important mechanisms that maintain amyloids at non-toxic levels *in vivo*. Amyloidosis occurring prior to reproduction will jeopardize survival of the species. Increased misfolded protein levels can be detected years prior to the appearance of disease symptoms (*e.g.* toxic Aβ oligomers in middle-aged humans (90) and particulate Aβ deposits in reproducing monkeys (91)). Moreover, young humans are susceptible to amyloidosis in conjunction with cardiovascular disease, infections, cancer, and exposure to environmental toxins (92–94) (*e.g.* atrial natriuretic peptide amyloidosis in congestive heart failure (95)). These arguments support the potential role of innate amyloid-clearing catabodies in furnishing an evolutionary survival advantage. Catabodies to the superantigens HIV gp120 (2, 96), *S. aureus* Efb (97), and *S. aureus* Protein A (present report) may serve as innate defense mediators against microbes. Superantigens, however, down-regulate acquired B- and T-cell immunity, and the survival

A

```
1.  TTR          61  FVEGI  65
    Aβ42         20  .A.DV  24

2.  TTR          52  LHGLTTEEEFV  62
    gp120       261  .N.SLA...V.  271

3.  TTR          99  WKALGISPFHE  109
    gp120        95  ..NNMVEQM..  106

4.  TTR          42  ASGKTSE  48
    Protein A   366  .NGT.AD  372
```

B

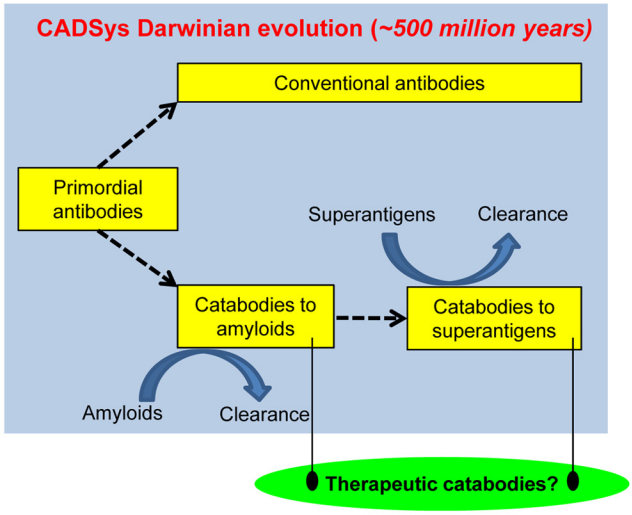

C

TTR

```
Homo sapiens          GTGESKCPLMVKVLDAVRGSPAINVAVHVFRKAADDTWEPFASGKTSESGELHGLTTEEEFVE
Leucoraja erinacea    .DHHTR..VLI.....LK.T..A..Q.QMLKRNE.K...TINT.V.GGN....N..S..HLAV

Homo sapiens          GIYKVEIDTKSYWKALGISPFHEHAEVVFTANDSGPRRYTIAALLSPYSYSTTAVVTNPKE
Leucoraja erinacea    .L..FHFE.GA..SNA.QAH...C.N...RVASLTSNH....V.........GIIM..HAT
```

Aβ

```
Homo sapiens          DAEFRHDSGYEVHHQKLVFFAEDVGSNKGAIIGLMVGGVVIA
Narke japonica        ET..QQ..............PK....................
```

FIGURE 8. **Catabody defense system (*CADSys*).** *A*, regions of TTR with the best sequence similarity to Aβ, gp120, and Protein A. *1*, TTR and Aβ42 ($e = 9.4$). *2* and *3*, TTR and gp120 ($e = 2.6$ and 6.4, respectively). *4*, TTR and Protein A ($e = 23$). *Dots*, identities. *Red*, conservative substitutions. Alignments were obtained with BLAST using the BLOSUM62 matrix and expect (*e*) threshold of 1,000. The sequence similarities are weak (large *e* values, $p > 0.05$ for all alignments). The indicated Protein A region, but not the Aβ42 and gp120 regions, has a β-turn-forming propensity. The TTR region aligned with Protein A also tends to form a β-turn. Substrate regions with the greatest β-turn forming propensity are as follows: TTR, 95–101 and 109–115; Aβ, 5–11 and 23–29; gp120, 146–147e and 362–368 (HXB2 numbering); Protein A, 259–265 and 299–305. Accession numbers are as follows: human TTR, AAA73473; human Aβ42, NP000475; HIV gp120MN, AF075721; *S. aureus* Protein A, 88193823. *B*, the catabody defense system concept is based on discovery of innate antibodies that clear pathogenic amyloids and microbial superantigens. Because amyloid removal is predicted to confer a survival advantage to the organism, the emergence of germ line anti-amyloid catabodies in immune evolution is proposed. Superantigen epitopes leave microbes susceptible to innate catabodies and reversibly binding antibodies. However, superantigens help microbes evade acquired immunity, and microbial superantigen-host immune system interactions probably reflect competing factors favoring survival of microbes and the host. *C*, amyloid protein conservation in humans and jawed fish of the Batoidea superorder (*Leucoraja erinacea* and *Narke japonica*). *Top*, TTR; *bottom*, Aβ42. *Dots*, amino acid identities. *Red*, conservative substitutions. The full-length human TTR and Aβ42 sequences are shown. Accession numbers are as follows: *L. erinacea* TTR, CV221819; *N. japonica* amyloid precursor protein 699 residues 601–642, BAA24230.1. Jawed fish are the first extant organisms with human antibody-like molecules.

advantage for the microbe gained by evading host acquired immunity (56) may trump the protective function of anti-superantigen catabodies.

In summary, our findings indicate the physiological production of misTTR-selective catabodies. Unlike other approaches to suppression of TTR amyloidosis, the catabodies remove misTTR without interfering in the essential functions of the properly folded TTR state. The misTTR-hydrolyzing IgMs, therefore, hold potential for developing a safe treatment for TTR amyloidosis. Several monoclonal IgMs have been approved in the United States for human tests, and pentamer IgM-containing polyclonal antibodies are approved for human therapy in Europe (98). Converting pentamer IgM to the monomer IgM state does not compromise the catalytic activity (1), and monomer IgMs can be considered as candidate therapeutic reagents. Small amounts of IgM monomers are found physiologically in humans (99), and lower organisms produce larger monomer IgM amounts (100). In addition, highly catalytic single V_L domains and paired V_L domains can be engineered (8, 29) as candidate drugs from the misTTR-hydrolyzing IgMs.

Acknowledgments—We thank Aubrey de Grey for comments and discussion and Heather Essigmann for assistance in sequence analysis. We thank Brian Poindexter for assistance in confocal microscopy studies. Flow cytometry was done at the Baylor College of Medicine Cytometry and Cell Sorting Core.

REFERENCES

1. Planque, S., Bangale, Y., Song, X. T., Karle, S., Taguchi, H., Poindexter, B., Bick, R., Edmundson, A., Nishiyama, Y., and Paul, S. (2004) Ontogeny of proteolytic immunity: IgM serine proteases. *J. Biol. Chem.* **279,** 14024–14032

2. Paul, S., Karle, S., Planque, S., Taguchi, H., Salas, M., Nishiyama, Y., Handy, B., Hunter, R., Edmundson, A., and Hanson, C. (2004) Naturally occurring proteolytic antibodies: selective immunoglobulin M-catalyzed hydrolysis of HIV gp120. *J. Biol. Chem.* **279,** 39611–39619
3. Gololobov, G., Sun, M., and Paul, S. (1999) Innate antibody catalysis. *Mol. Immunol.* **36,** 1215–1222
4. Sharma, V., Heriot, W., Trisler, K., and Smider, V. (2009) A human germ line antibody light chain with hydrolytic properties associated with multimerization status. *J. Biol. Chem.* **284,** 33079–33087
5. Hifumi, E., Honjo, E., Fujimoto, N., Arakawa, M., Nishizono, A., and Uda, T. (2012) Highly efficient method of preparing human catalytic antibody light chains and their biological characteristics. *FASEB J.* **26,** 1607–1615
6. Le Minoux, D., Mahendra, A., Kaveri, S., Limnios, N., Friboulet, A., Avalle, B., Boquet, D., Lacroix-Desmazes, S., and Padiolleau-Lefèvre, S. (2012) A novel molecular analysis of genes encoding catalytic antibodies. *Mol. Immunol.* **50,** 160–168
7. Taguchi, H., Planque, S., Nishiyama, Y., Symersky, J., Boivin, S., Szabo, P., Friedland, R. P., Ramsland, P. A., Edmundson, A. B., Weksler, M. E., and Paul, S. (2008) Autoantibody-catalyzed hydrolysis of amyloid β peptide. *J. Biol. Chem.* **283,** 4714–4722
8. Paul, S., Planque, S. A., Nishiyama, Y., Hanson, C. V., and Massey, R. J. (2012) Nature and nurture of catalytic antibodies. *Adv. Exp. Med. Biol.* **750,** 56–75
9. Paul, S., Volle, D. J., Beach, C. M., Johnson, D. R., Powell, M. J., and Massey, R. J. (1989) Catalytic hydrolysis of vasoactive intestinal peptide by human autoantibody. *Science* **244,** 1158–1162
10. Shuster, A. M., Gololobov, G. V., Kvashuk, O. A., Bogomolova, A. E., Smirnov, I. V., and Gabibov, A. G. (1992) DNA hydrolyzing autoantibodies. *Science* **256,** 665–667
11. Buxbaum, J. N. (2003) Diseases of protein conformation: what do *in vitro* experiments tell us about *in vivo* diseases? *Trends Biochem. Sci.* **28,** 585–592
12. Buxbaum, J. N., and Reixach, N. (2009) Transthyretin: the servant of many masters. *Cell Mol. Life Sci.* **66,** 3095–3101
13. Takeuchi, M., Mizuguchi, M., Kouno, T., Shinohara, Y., Aizawa, T., Demura, M., Mori, Y., Shinoda, H., and Kawano, K. (2007) Destabilization of transthyretin by pathogenic mutations in the DE loop. *Proteins* **66,** 716–725
14. Quintas, A., Vaz, D. C., Cardoso, I., Saraiva, M. J., and Brito, R. M. (2001) Tetramer dissociation and monomer partial unfolding precedes protofibril formation in amyloidogenic transthyretin variants. *J. Biol. Chem.* **276,** 27207–27213
15. Hurshman, A. R., White, J. T., Powers, E. T., and Kelly, J. W. (2004) Transthyretin aggregation under partially denaturing conditions is a downhill polymerization. *Biochemistry* **43,** 7365–7381
16. Kingsbury, J. S., Laue, T. M., Chase, S. F., and Connors, L. H. (2012) Detection of high-molecular-weight amyloid serum protein complexes using biological on-line tracer sedimentation. *Anal. Biochem.* **425,** 151–156
17. Sueyoshi, T., Ueda, M., Jono, H., Irie, H., Sei, A., Ide, J., Ando, Y., and Mizuta, H. (2011) Wild-type transthyretin-derived amyloidosis in various ligaments and tendons. *Hum. Pathol.* **42,** 1259–1264
18. Pepys, M. B. (2006) Amyloidosis. *Annu. Rev. Med.* **57,** 223–241
19. Westermark, P., Bergström, J., Solomon, A., Murphy, C., and Sletten, K. (2003) Transthyretin-derived senile systemic amyloidosis: clinicopathologic and structural considerations. *Amyloid* **10,** 48–54
20. Teixeira, P. F., Cerca, F., Santos, S. D., and Saraiva, M. J. (2006) Endoplasmic reticulum stress associated with extracellular aggregates. Evidence from transthyretin deposition in familial amyloid polyneuropathy. *J. Biol. Chem.* **281,** 21998–22003
21. Connors, L. H., Lim, A., Prokaeva, T., Roskens, V. A., and Costello, C. E. (2003) Tabulation of human transthyretin (TTR) variants. *Amyloid* **10,** 160–184
22. Coelho, T., Adams, D., Silva, A., Lozeron, P., Hawkins, P. N., Mant, T., Perez, J., Chiesa, J., Warrington, S., Tranter, E., Munisamy, M., Falzone, R., Harrop, J., Cehelsky, J., Bettencourt, B. R., Geissler, M., Butler, J. S., Sehgal, A., Meyers, R. E., Chen, Q., Borland, T., Hutabarat, R. M., Clausen, V. A., Alvarez, R., Fitzgerald, K., Gamba-Vitalo, C., Nochur, S. V., Vaishnaw, A. K., Sah, D. W., Gollob, J. A., and Suhr, O. B. (2013) Safety and efficacy of RNAi therapy for transthyretin amyloidosis. *N. Engl. J. Med.* **369,** 819–829
23. Coelho, T., Maia, L. F., Martins da Silva, A., Waddington Cruz, M., Planté-Bordeneuve, V., Lozeron, P., Suhr, O. B., Campistol, J. M., Conceição, I. M., Schmidt, H. H., Trigo, P., Kelly, J. W., Labaudinière, R., Chan, J., Packman, J., Wilson, A., and Grogan, D. R. (2012) Tafamidis for transthyretin familial amyloid polyneuropathy: a randomized, controlled trial. *Neurology* **79,** 785–792
24. Salloway, S., Sperling, R., Fox, N. C., Blennow, K., Klunk, W., Raskind, M., Sabbagh, M., Honig, L. S., Porsteinsson, A. P., Ferris, S., Reichert, M., Ketter, N., Nejadnik, B., Guenzler, V., Miloslavsky, M., Wang, D., Lu, Y., Lull, J., Tudor, I. C., Liu, E., Grundman, M., Yuen, E., Black, R., and Brashear, H. R. (2014) Two phase 3 trials of bapineuzumab in mild-to-moderate Alzheimer's disease. *N. Engl. J. Med.* **370,** 322–333
25. Su, Y., Jono, H., Torikai, M., Hosoi, A., Soejima, K., Guo, J., Tasaki, M., Misumi, Y., Ueda, M., Shinriki, S., Shono, M., Obayashi, K., Nakashima, T., Sugawara, K., and Ando, Y. (2012) Antibody therapy for familial amyloidotic polyneuropathy. *Amyloid* **19,** 45–46
26. Lindström, V., Ihse, E., Fagerqvist, T., Bergström, J., Nordström, E., Möller, C., Lannfelt, L., and Ingelsson, M. (2014) Immunotherapy targeting α-synuclein, with relevance for future treatment of Parkinson's disease and other Lewy body disorders. *Immunotherapy* **6,** 141–153
27. Mitsuda, Y., Planque, S., Hara, M., Kyle, R., Taguchi, H., Nishiyama, Y., and Paul, S. (2007) Naturally occurring catalytic antibodies: evidence for preferred development of the catalytic function in IgA class antibodies. *Mol. Biotechnol.* **36,** 113–122
28. Sapparapu, G., Planque, S., Mitsuda, Y., McLean, G., Nishiyama, Y., and Paul, S. (2012) Constant domain-regulated antibody catalysis. *J. Biol. Chem.* **287,** 36096–36104
29. Taguchi, H., Planque, S., Sapparapu, G., Boivin, S., Hara, M., Nishiyama, Y., and Paul, S. (2008) Exceptional amyloid β peptide hydrolyzing activity of nonphysiological immunoglobulin variable domain scaffolds. *J. Biol. Chem.* **283,** 36724–36733
30. Lundberg, E., Olofsson, A., Westermark, G. T., and Sauer-Eriksson, A. E. (2009) Stability and fibril formation properties of human and fish transthyretin, and of the *Escherichia coli* transthyretin-related protein. *FEBS J.* **276,** 1999–2011
31. Yang, D. T., Joshi, G., Cho, P. Y., Johnson, J. A., and Murphy, R. M. (2013) Transthyretin as both a sensor and a scavenger of β-amyloid oligomers. *Biochemistry* **52,** 2849–2861
32. Xia, K., Zhang, S., Bathrick, B., Liu, S., Garcia, Y., and Colón, W. (2012) Quantifying the kinetic stability of hyperstable proteins via time-dependent SDS trapping. *Biochemistry* **51,** 100–107
33. Paul, S., Planque, S., Zhou, Y. X., Taguchi, H., Bhatia, G., Karle, S., Hanson, C., and Nishiyama, Y. (2003) Specific HIV gp120-cleaving antibodies induced by covalently reactive analog of gp120. *J. Biol. Chem.* **278,** 20429–20435
34. Beynon, R. J., and Salvesen, G. S. (2001) in *Proteolytic Enzymes: A Practical Approach*, 2nd Ed. (Beynon, R. J., and Bond, J. S., eds) pp. 317–330, Oxford University Press, Oxford, UK
35. Paul, S., Tramontano, A., Gololobov, G., Zhou, Y. X., Taguchi, H., Karle, S., Nishiyama, Y., Planque, S., and George, S. (2001) Phosphonate ester probes for proteolytic antibodies. *J. Biol. Chem.* **276,** 28314–28320
36. Sousa, M. M., do Amaral, J. B., Guimarães, A., and Saraiva, M. J. (2005) Up-regulation of the extracellular matrix remodeling genes, biglycan, neutrophil gelatinase-associated lipocalin, and matrix metalloproteinase-9 in familial amyloid polyneuropathy. *FASEB J.* **19,** 124–126
37. Mody, R., Tramontano, A., and Paul, S. (1994) Spontaneous hydrolysis of vasoactive intestinal peptide in neutral aqueous solution. *Int. J. Pept. Protein Res.* **44,** 441–447
38. Reixach, N., Deechongkit, S., Jiang, X., Kelly, J. W., and Buxbaum, J. N. (2004) Tissue damage in the amyloidoses: transthyretin monomers and nonnative oligomers are the major cytotoxic species in tissue culture. *Proc. Natl. Acad. Sci. U.S.A.* **101,** 2817–2822
39. Sörgjerd, K., Klingstedt, T., Lindgren, M., Kågedal, K., and Hammarström, P. (2008) Prefibrillar transthyretin oligomers and cold stored native tetrameric transthyretin are cytotoxic in cell culture. *Biochem.*

Biophys. Res. Commun. **377,** 1072–1078
40. Takeshita, S., Tokutomi, T., Kawase, H., Nakatani, K., Tsujimoto, H., Kawamura, Y., and Sekine, I. (2001) Elevated serum levels of matrix metalloproteinase-9 (MMP-9) in Kawasaki disease. *Clin. Exp. Immunol.* **125,** 340–344
41. Chen, T. Y., Huang, C. C., and Tsao, C. J. (1993) Hemostatic molecular markers in nephrotic syndrome. *Am. J. Hematol.* **44,** 276–279
42. Foguel, D., Suarez, M. C., Ferrão-Gonzales, A. D., Porto, T. C., Palmieri, L., Einsiedler, C. M., Andrade, L. R., Lashuel, H. A., Lansbury, P. T., Kelly, J. W., and Silva, J. L. (2003) Dissociation of amyloid fibrils of α-synuclein and transthyretin by pressure reveals their reversible nature and the formation of water-excluded cavities. *Proc. Natl. Acad. Sci. U.S.A.* **100,** 9831–9836
43. Gao, Q. S., Sun, M., Rees, A. R., and Paul, S. (1995) Site-directed mutagenesis of proteolytic antibody light chain. *J. Mol. Biol.* **253,** 658–664
44. Polosukhina, D. I., Kanyshkova, T. G., Doronin, B. M., Tyshkevich, O. B., Buneva, V. N., Boiko, A. N., Gusev, E. I., Nevinsky, G. A., and Favorova, O. O. (2006) Metal-dependent hydrolysis of myelin basic protein by IgGs from the sera of patients with multiple sclerosis. *Immunol. Lett.* **103,** 75–81
45. Baranova, S. V., Buneva, V. N., Kharitonova, M. A., Sizyakina, L. P., Calmels, C., Andreola, M. L., Parissi, V., Zakharova, O. D., and Nevinsky, G. A. (2010) HIV-1 integrase-hydrolyzing IgM antibodies from sera of HIV-infected patients. *Int. Immunol.* **22,** 671–680
46. Kalaga, R., Li, L., O'Dell, J. R., and Paul, S. (1995) Unexpected presence of polyreactive catalytic antibodies in IgG from unimmunized donors and decreased levels in rheumatoid arthritis. *J. Immunol.* **155,** 2695–2702
47. Schurr, J. M., and McLaren, A. D. (1966) Enzyme action: comparison on soluble and insoluble substrate. *Science* **152,** 1064–1066
48. Cruys-Bagger, N., Elmerdahl, J., Praestgaard, E., Borch, K., and Westh, P. (2013) A steady-state theory for processive cellulases. *FEBS J.* **280,** 3952–3961
49. Paul, S., Volle, D. J., Powell, M. J., and Massey, R. J. (1990) Site specificity of a catalytic vasoactive intestinal peptide antibody. An inhibitory vasoactive intestinal peptide subsequence distant from the scissile peptide bond. *J. Biol. Chem.* **265,** 11910–11913
50. Planque, S., Taguchi, H., Burr, G., Bhatia, G., Karle, S., Zhou, Y. X., Nishiyama, Y., and Paul, S. (2003) Broadly distributed chemical reactivity of natural antibodies expressed in coordination with specific antigen binding activity. *J. Biol. Chem.* **278,** 20436–20443
51. Casali, P., and Schettino, E. W. (1996) Structure and function of natural antibodies. *Curr. Top. Microbiol. Immunol.* **210,** 167–179
52. O'Nuallain, B., and Wetzel, R. (2002) Conformational Abs recognizing a generic amyloid fibril epitope. *Proc. Natl. Acad. Sci. U.S.A.* **99,** 1485–1490
53. Kayed, R., Head, E., Thompson, J. L., McIntire, T. M., Milton, S. C., Cotman, C. W., and Glabe, C. G. (2003) Common structure of soluble amyloid oligomers implies common mechanism of pathogenesis. *Science* **300,** 486–489
54. Graille, M., Stura, E. A., Corper, A. L., Sutton, B. J., Taussig, M. J., Charbonnier, J. B., and Silverman, G. J. (2000) Crystal structure of a *Staphylococcus aureus* protein A domain complexed with the Fab fragment of a human IgM antibody: structural basis for recognition of B-cell receptors and superantigen activity. *Proc. Natl. Acad. Sci. U.S.A.* **97,** 5399–5404
55. Neshat, M. N., Goodglick, L., Lim, K., and Braun, J. (2000) Mapping the B cell superantigen binding site for HIV-1 gp120 on a V(H)3 Ig. *Int. Immunol.* **12,** 305–312
56. Goodyear, C. S., and Silverman, G. J. (2005) B cell superantigens: a microbe's answer to innate-like B cells and natural antibodies. *Springer Semin. Immunopathol.* **26,** 463–484
57. Nishiyama, Y., Planque, S., Mitsuda, Y., Nitti, G., Taguchi, H., Jin, L., Symersky, J., Boivin, S., Sienczyk, M., Salas, M., Hanson, C. V., and Paul, S. (2009) Toward effective HIV vaccination: induction of binary epitope reactive antibodies with broad HIV neutralizing activity. *J. Biol. Chem.* **284,** 30627–30642
58. Planque, S. A., Mitsuda, Y., Nishiyama, Y., Karle, S., Boivin, S., Salas, M., Morris, M. K., Hara, M., Liao, G., Massey, R. J., Hanson, C. V., and Paul, S. (2012) Antibodies to a superantigenic glycoprotein 120 epitope as the basis for developing an HIV vaccine. *J. Immunol.* **189,** 5367–5381
59. Spencer, J., and Hall, J. G. (1984) The flow and composition of lymph from the caudal mediastinal lymph node of sheep. *Immunology* **52,** 7–15
60. Rossing, N. (1978) Intra- and extravascular distribution of albumin and immunoglobulin in man. *Lymphology* **11,** 138–142
61. Pilati, C. F. (1990) Macromolecular transport in canine coronary microvasculature. *Am. J. Physiol.* **258,** H748–H753
62. Gomes, R., Sousa Silva, M., Quintas, A., Cordeiro, C., Freire, A., Pereira, P., Martins, A., Monteiro, E., Barroso, E., and Ponces Freire, A. (2005) Argpyrimidine, a methylglyoxal-derived advanced glycation end-product in familial amyloidotic polyneuropathy. *Biochem. J.* **385,** 339–345
63. Liu, L., Komatsu, H., Murray, I. V., and Axelsen, P. H. (2008) Promotion of amyloid β protein misfolding and fibrillogenesis by a lipid oxidation product. *J. Mol. Biol.* **377,** 1236–1250
64. Wang, X., and Stollar, B. D. (1999) Immunoglobulin VH gene expression in human aging. *Clin. Immunol.* **93,** 132–142
65. Gibson, K. L., Wu, Y. C., Barnett, Y., Duggan, O., Vaughan, R., Kondeatis, E., Nilsson, B. O., Wikby, A., Kipling, D., and Dunn-Walters, D. K. (2009) B-cell diversity decreases in old age and is correlated with poor health status. *Aging Cell* **8,** 18–25
66. Gavazzi, G., and Krause, K. H. (2002) Ageing and infection. *Lancet Infect. Dis.* **2,** 659–666
67. Maas, A., Dingjan, G. M., Grosveld, F., and Hendriks, R. W. (1999) Early arrest in B cell development in transgenic mice that express the E41K Bruton's tyrosine kinase mutant under the control of the CD19 promoter region. *J. Immunol.* **162,** 6526–6533
68. Conley, M. E., Dobbs, A. K., Farmer, D. M., Kilic, S., Paris, K., Grigoriadou, S., Coustan-Smith, E., Howard, V., and Campana, D. (2009) Primary B cell immunodeficiencies: comparisons and contrasts. *Annu. Rev. Immunol.* **27,** 199–227
69. Liu, Y. H., Giunta, B., Zhou, H. D., Tan, J., and Wang, Y. J. (2012) Immunotherapy for Alzheimer disease: the challenge of adverse effects. *Nat. Rev. Neurol.* **8,** 465–469
70. Pollack, S. J., Hsiun, P., and Schultz, P. G. (1989) Stereospecific hydrolysis of alkyl esters by antibodies. *J. Am. Chem. Soc.* **111,** 5961–5962
71. Ramsland, P. A., Terzyan, S. S., Cloud, G., Bourne, C. R., Farrugia, W., Tribbick, G., Geysen, H. M., Moomaw, C. R., Slaughter, C. A., and Edmundson, A. B. (2006) Crystal structure of a glycosylated Fab from an IgM cryoglobulin with properties of a natural proteolytic antibody. *Biochem. J.* **395,** 473–481
72. Janda, A., Eryilmaz, E., Nakouzi, A., Cowburn, D., and Casadevall, A. (2012) Variable region identical immunoglobulins differing in isotype express different paratopes. *J. Biol. Chem.* **287,** 35409–35417
73. Haury, M., Sundblad, A., Grandien, A., Barreau, C., Coutinho, A., and Nobrega, A. (1997) The repertoire of serum IgM in normal mice is largely independent of external antigenic contact. *Eur. J. Immunol.* **27,** 1557–1563
74. Köhler, F., Hug, E., Eschbach, C., Meixlsperger, S., Hobeika, E., Kofer, J., Wardemann, H., and Jumaa, H. (2008) Autoreactive B cell receptors mimic autonomous pre-B cell receptor signaling and induce proliferation of early B cells. *Immunity* **29,** 912–921
75. Nissim, A., and Chernajovsky, Y. (2008) in *Therapeutic Antibodies: Handbook of Experimental Pharmacology* (Chernajovsky, Y., and Nissim, A., eds) pp. 3–18, Springer, Berlin
76. Ponomarenko, N. A., Durova, O. M., Vorobiev, I. I., Belogurov, A. A., Jr., Kurkova, I. N., Petrenko, A. G., Telegin, G. B., Suchkov, S. V., Kiselev, S. L., Lagarkova, M. A., Govorun, V. M., Serebryakova, M. V., Avalle, B., Tornatore, P., Karavanov, A., Morse, H. C., 3rd, Thomas, D., Friboulet, A., and Gabibov, A. G. (2006) Autoantibodies to myelin basic protein catalyze site-specific degradation of their antigen. *Proc. Natl. Acad. Sci. U.S.A.* **103,** 281–286
77. Wootla, B., Dasgupta, S., Dimitrov, J. D., Bayry, J., Lévesque, H., Borg, J. Y., Borel-Derlon, A., Rao, D. N., Friboulet, A., Kaveri, S. V., and Lacroix-Desmazes, S. (2008) Factor VIII hydrolysis mediated by anti-factor VIII autoantibodies in acquired hemophilia. *J. Immunol.* **180,** 7714–7720
78. Wootla, B., Christophe, O. D., Mahendra, A., Dimitrov, J. D., Repessé, Y., Ollivier, V., Friboulet, A., Borel-Derlon, A., Levesque, H., Borg, J. Y., Andre, S., Bayry, J., Calvez, T., Kaveri, S. V., and Lacroix-Desmazes, S.

(2011) Proteolytic antibodies activate factor IX in patients with acquired hemophilia. *Blood* **117,** 2257–2264
79. Andrievskaya, O. A., Buneva, V. N., Naumov, V. A., and Nevinsky, G. A. (2000) Catalytic heterogenity of polyclonal RNA-hydrolyzing IgM from sera of patients with lupus erythematosus. *Med. Sci. Monit.* **6,** 460–470
80. Saveliev, A. N., Ivanen, D. R., Kulminskaya, A. A., Ershova, N. A., Kanyshkova, T. G., Buneva, V. N., Mogelnitskii, A. S., Doronin, B. M., Favorova, O. O., Nevinsky, G. A., and Neustroev, K. N. (2003) Amylolytic activity of IgM and IgG antibodies from patients with multiple sclerosis. *Immunol. Lett.* **86,** 291–297
81. Gao, Q. S., Sun, M., Tyutyulkova, S., Webster, D., Rees, A., Tramontano, A., Massey, R. J., and Paul, S. (1994) Molecular cloning of a proteolytic antibody light chain. *J. Biol. Chem.* **269,** 32389–32393
82. Uda, T., and Hifumi, E. (2004) Super catalytic antibody and antigenase. *J. Biosci. Bioeng.* **97,** 143–152
83. Hifumi, E., Morihara, F., Hatiuchi, K., Okuda, T., Nishizono, A., and Uda, T. (2008) Catalytic features and eradication ability of antibody light-chain UA15-L against *Helicobacter pylori*. *J. Biol. Chem.* **283,** 899–907
84. Coutinho, A., Kazatchkine, M. D., and Avrameas, S. (1995) Natural autoantibodies. *Curr. Opin. Immunol.* **7,** 812–818
85. Bayry, J., Misra, N., Dasgupta, S., Lacroix-Desmazes, S., Kazatchkine, M. D., and Kaveri, S. V. (2005) Natural autoantibodies: immune homeostasis and therapeutic intervention. *Expert Rev. Clin. Immunol.* **1,** 213–222
86. Kaveri, S. V. (2012) Intravenous immunoglobulin: exploiting the potential of natural antibodies. *Autoimmun. Rev.* **11,** 792–794
87. Kohler, H., and Paul, S. (1998) Superantibody activities: new players in innate and adaptive immune responses. *Immunol. Today* **19,** 221–227
88. Graille, M., Harrison, S., Crump, M. P., Findlow, S. C., Housden, N. G., Muller, B. H., Battail-Poirot, N., Sibaï, G., Sutton, B. J., Taussig, M. J., Jolivet-Reynaud, C., Gore, M. G., and Stura, E. A. (2002) Evidence for plasticity and structural mimicry at the immunoglobulin light chain-protein L interface. *J. Biol. Chem.* **277,** 47500–47506
89. Maftei, M., Thurm, F., Leirer, V. M., von Arnim, C. A., Elbert, T., Przybylski, M., Kolassa, I. T., and Manea, M. (2012) Antigen-bound and free β-amyloid autoantibodies in serum of healthy adults. *PLoS One* **7,** e44516
90. Lesné, S. E., Sherman, M. A., Grant, M., Kuskowski, M., Schneider, J. A., Bennett, D. A., and Ashe, K. H. (2013) Brain amyloid-β oligomers in ageing and Alzheimer's disease. *Brain* **136,** 1383–1398
91. Kalinin, S., Willard, S. L., Shively, C. A., Kaplan, J. R., Register, T. C., Jorgensen, M. J., Polak, P. E., Rubinstein, I., and Feinstein, D. L. (2013) Development of amyloid burden in African Green monkeys. *Neurobiol. Aging* **34,** 2361–2369
92. Lane, T., Loeffler, J. M., Rowczenio, D. M., Gilbertson, J. A., Bybee, A., Russell, T. L., Gillmore, J. D., Wechalekar, A. D., Hawkins, P. N., and Lachmann, H. J. (2013) AA amyloidosis complicating the hereditary periodic fever syndromes. *Arthritis Rheum.* **65,** 1116–1121
93. Abdallah, E., and Waked, E. (2013) Incidence and clinical outcome of renal amyloidosis: a retrospective study. *Saudi J. Kidney Dis. Transpl.* **24,** 950–958
94. Calderón-Garciduenas, L., Franco-Lira, M., Mora-Tiscareño, A., Medina-Cortina, H., Torres-Jardón, R., and Kavanaugh, M. (2013) Early Alzheimer's and Parkinson's disease pathology in urban children: friend *versus* foe responses: it is time to face the evidence. *Biomed. Res. Int.* **2013,** 161687
95. Millucci, L., Ghezzi, L., Bernardini, G., Braconi, D., Tanganelli, P., and Santucci, A. (2012) Prevalence of isolated atrial amyloidosis in young patients affected by congestive heart failure. *Scientific World Journal* **2012,** 293863
96. Planque, S., Mitsuda, Y., Taguchi, H., Salas, M., Morris, M. K., Nishiyama, Y., Kyle, R., Okhuysen, P., Escobar, M., Hunter, R., Sheppard, H. W., Hanson, C., and Paul, S. (2007) Characterization of gp120 hydrolysis by IgA antibodies from humans without HIV infection. *AIDS Res. Hum. Retroviruses* **23,** 1541–1554
97. Brown, E. L., Nishiyama, Y., Dunkle, J. W., Aggarwal, S., Planque, S., Watanabe, K., Csencsits-Smith, K., Bowden, M. G., Kaplan, S. L., and Paul, S. (2012) Constitutive production of catalytic antibodies to a *Staphylococcus aureus* virulence factor and effect of infection. *J. Biol. Chem.* **287,** 9940–9951
98. Kreymann, K. G., de Heer, G., Nierhaus, A., and Kluge, S. (2007) Use of polyclonal immunoglobulins as adjunctive therapy for sepsis or septic shock. *Crit. Care Med.* **35,** 2677–2685
99. Xu, H. J., Umapathysivam, K., McNeilage, J., Gordon, T. P., and Roberts-Thomson, P. J. (1992) An enhanced chemiluminescence detection system combined with a modified immunoblot technique for the detection of low molecular weight IgM in sera from healthy adults and neonates. *J. Immunol. Methods* **146,** 241–247
100. Dooley, H., and Flajnik, M. F. (2006) Antibody repertoire development in cartilaginous fish. *Dev. Comp. Immunol.* **30,** 43–56